New spacetime discontinuous Galerkin methods for solving convection-diffusion systems

S. May

_____

New spacetime discontinuous Galerkin methods for solving convection-diffusion systems[*]

Sandra May[†]

In this paper, we present two new methods for solving systems of hyperbolic conservation laws with correct physical viscosity and heat conduction terms. In particular we are interested in solving the compressible Navier-Stokes equations. Both methods are extensions of the spacetime discontinuous Galerkin method for hyperbolic conservation laws developed by Hiltebrand and Mishra [17]. Following this work, we use entropy variables as degrees of freedom and entropy stable finite volume fluxes. For the discretization of the diffusion term, we consider two different approaches: the interior penalty approach and a variant of the local discontinuous Galerkin method. For both approaches we show an entropy stability estimate. We also present numerical results in one dimension comparing both methods.

1. Introduction

Over the past decade, discontinuous Galerkin (DG) methods have become increasingly popular for solving nonlinear partial differential equations (PDEs) such as systems of conservation laws. One reason for this development is the fact that DG methods, as compared to finite volume methods, are more suitable for deducing theoretical stability or convergence results. Another reason is that DG methods operate very locally, even for high-order methods. This makes them a good fit for modern supercomputers. However, many theoretical stability results for DG methods only exist for the case of scalar equations. For systems of conservation laws, like the compressible Euler equations, there are significantly fewer results available, especially for the case of a fully discrete method.

In [17], Hiltebrand and Mishra developed a spacetime DG method for solving systems of conservation laws based on using entropy variables instead of the standard conservative variables. The scheme uses entropy stable fluxes and features a streamline diffusion and a shock capturing term to handle the shocks and discontinuities occurring in the solution of the system. The scheme has several desirable features: it is (arbitrarily) high order, unconditionally stable, it works in multiple dimensions on unstructured grids, it is fully discrete, and one can show a priori entropy stability estimates for the fully discrete scheme for systems of conservation laws.

Therefore, the scheme combines theoretical stability properties for systems of conservation laws with good performance properties in the actual computation of the numerical solutions.

The goal of this work is to extend the scheme developed in [17] from systems of conservation laws to convection-diffusion systems *while preserving* these desirable properties. In particular, we are interested in solving the compressible Navier-Stokes equations where physical viscosity and heat conduction are added to the compressible Euler equations.

In our extension of the original scheme, we consider two approaches for incorporating the viscous terms:

1. an approach based on the interior penalty (IP) method introduced by Arnold [1] resulting in the ST-IP-DG method;

2. an approach in the spirit of the local discontinuous Galerkin (LDG) method introduced by Cockburn and Shu [7] resulting in the ST-LDG method.

For both methods, we will deduce an entropy stability estimate for convection-diffusion systems under suitable assumptions.

In the literature, there are various DG methods for solving the compressible Navier-Stokes equations, all of them based on discretizing the conserved variables of the system. One of the first successful attempts was made by Bassi and Rebay [4, 5]. The authors solved the equations numerically but do not provide any theoretical considerations for their scheme. In [7], Cockburn and Shu developed the LDG method for convection-diffusion systems. The authors extended Bassis and Rebay's approach of writing the equations as a first-order system to general systems of convection-diffusion equations and provide stability estimates for the case of the diffusion term being elliptic. However, only numerical results for the linear advection-diffusion equation are contained in this work.

In the following, several authors have developed versions of the LDG method that are more compact in multiple space dimensions [22, 6] and have applied these versions successfully to solve the compressible Navier-Stokes equations [23, 6]. However, to the best of our knowledge, there are no stability results for a fully discrete method for approximating the Navier-Stokes equations. Existing stability results are typically limited to the case of an elliptic diffusion operator.

Another approach for solving the compressible Navier-Stokes equations is based on the IP method. Recent work includes the work by Hartmann and Houston [14, 15]. However, like for the LDG approaches, stability results are only available for the case of elliptic diffusion operators. A unified comparison of the various methods mentioned above for the case of elliptic operators can be found in [2].

Though significantly less extensive, there is also some literature for solving the compressible Navier-Stokes equations using entropy variables as degrees of freedom. Early work has been done by Shakib et al. [25]. The authors use a finite element formulation and show theoretical stability estimates as well as numerical results. Different to our method, the authors use continuous elements in space and a discontinuous approach in time. Tadmor and Zhong [27] have developed a difference scheme based on entropy variables. The scheme uses entropy conservative fluxes for the non-linear term and centered differences for the discretization of the dissipation term. The authors show entropy stability for the semi-discrete form as well as numerical results. Even though both works have some features in common with the methods presented here, there are also significant differences.

This paper is structured as follows: we start with a review of the original method for conservation laws [17] in Section 2. Then, in Section 3, we discuss the effect of switching to entropy variables on the diffusion matrix. In Sections 4 and 5, we present our two different extensions, the ST-IP-DG and the ST-LDG method, and prove an entropy stability estimate for both methods under suitable assumptions. In Section 6, we show numerical results in one space dimension for both methods. In particular, we solve the compressible Navier-Stokes equations. We conclude this work with a comparison of both methods in Section 7.

2. Review of the spacetime DG method for hyperbolic systems

In this section, we review the spacetime DG method developed for hyperbolic conservation laws [17] that our method is based on. We focus on systems of conservation laws in one dimension given by

$$\mathbf{U}_t + \mathbf{F}(\mathbf{U})_x = 0. \tag{1}$$

Here, $\mathbf{U} : \Omega \subset \mathbb{R} \to \mathbb{R}^m, m \in \mathbb{N}$, is the vector of conserved variables and $\mathbf{F}$ is the flux vector. Assuming a strictly convex entropy function S, the map $\mathbf{U} \to \mathbf{V}$ is one-to-one, where $\mathbf{V} = S_{\mathbf{U}}(\mathbf{U})$ denotes the entropy variables. Therefore, we can equivalently write the system as

$$\mathbf{U}(\mathbf{V})_t + \mathbf{F}(\mathbf{V})_x = 0 \tag{2}$$

with $\mathbf{F}(\mathbf{V}) = \mathbf{F}(\mathbf{U}(\mathbf{V}))$ for simplicity. To discretize, we consider a spacetime grid with each spacetime element being a tensor-product of a spatial grid cell $K_i = [x_{i-1/2}, x_{i+1/2}] \subset \Omega$ and a time segment $I^n = [t^n, t^{n+1}] \subset [0, T]$. Then, approximations $\mathbf{V}^{\Delta x} = (v_1^{\Delta x}, \ldots, v_m^{\Delta x})^T$ to the solution $\mathbf{V}$ are sought in the space

$$\mathbf{V}^{\Delta x} \in \mathcal{V}^k = \left\{ \mathbf{\Phi}^{\Delta x} \in (L^1(\Omega \times [0, T]))^m \ : \ \begin{array}{l} \mathbf{\Phi}^{\Delta x}|_{K_i \times I^n} \text{ is a polynomial} \\ \text{of degree } k \text{ in each component} \end{array} \right\}.$$

Multiplying (2) with test functions $\mathbf{\Phi}^{\Delta x}$, integrating in space and time, and doing integration by parts with using numerical fluxes where appropriate results in

$$
\begin{aligned}
\mathcal{B}_{\mathrm{DG}}(\mathbf{V}^{\Delta x}, \mathbf{\Phi}^{\Delta x}) = \\
&- \sum_{n,i} \int_{I^n} \int_{K_i} \left(\langle \mathbf{U}(\mathbf{V}^{\Delta x}), \mathbf{\Phi}_t^{\Delta x} \rangle + \langle \mathbf{F}(\mathbf{V}^{\Delta x}), \mathbf{\Phi}_x^{\Delta x} \rangle \right) \, dx \, dt \\
&+ \sum_{n,i} \int_{K_i} \left(\langle \mathbb{U}(\mathbf{V}_{n+1,-}^{\Delta x}, \mathbf{V}_{n+1,+}^{\Delta x}), \mathbf{\Phi}_{n+1,-}^{\Delta x} \rangle - \langle \mathbb{U}(\mathbf{V}_{n,-}^{\Delta x}, \mathbf{V}_{n,+}^{\Delta x}), \mathbf{\Phi}_{n,+}^{\Delta x} \rangle \right) \, dx \\
&+ \sum_{n,i} \int_{I^n} \left(\langle \mathbb{F}(\mathbf{V}_{i+1/2,L}^{\Delta x}, \mathbf{V}_{i+1/2,R}^{\Delta x}), \mathbf{\Phi}_{i+1/2,L}^{\Delta x} \rangle - \langle \mathbb{F}(\mathbf{V}_{i-1/2,L}^{\Delta x}, \mathbf{V}_{i-1/2,R}^{\Delta x}), \mathbf{\Phi}_{i-1/2,R}^{\Delta x} \rangle \right) \, dt.
\end{aligned}
\tag{3}
$$

Here, $\langle \cdot, \cdot \rangle$ denotes the standard scalar product $\langle \mathbf{V}^{\Delta x}, \mathbf{\Phi}^{\Delta x} \rangle = \sum_{j=1}^m v_j^{\Delta x} \Phi_j^{\Delta x}$ and the indices $+/-$ and L/R denote the following limits

$$v_{n+1,\pm}^{\Delta x}(x) = \lim_{h \to 0} v^{\Delta x}(x, t^{n+1} \pm h), \quad v_{i+1/2,R/L}^{\Delta x}(t) = \lim_{h \to 0} v^{\Delta x}(x_{i+1/2} \pm h, t).$$

Furthermore, $\mathbb{U}$ and $\mathbb{F}$ denote the fluxes in time and space. In order to enable proper time marching, the upwind flux is chosen in time, i.e.,

$$\mathbb{U}(\mathbf{V}_{n+1,-}^{\Delta x}, \mathbf{V}_{n+1,+}^{\Delta x}) = \mathbf{U}(\mathbf{V}_{n+1,-}^{\Delta x}).$$

3

For the numerical flux in space either an entropy conservative flux or an entropy stable flux is used. Entropy conservative fluxes $\mathbb{F}^*$ have been examined in [26] and satisfy

$$\langle b - a, \mathbb{F}^*(a, b) \rangle = \psi(b) - \psi(a) \tag{4}$$

with $\psi = \langle \mathbf{V}, \mathbf{F} \rangle - Q$ being the entropy potential and Q being the entropy flux function corresponding to S. (We will specify the entropy conservative fluxes that we use for numerical tests in the corresponding parts of Section 6.)

Entropy stable fluxes are created out of entropy conservative fluxes by adding a diffusion term

$$\mathbb{F}(\mathbf{V}_a^{\Delta x}, \mathbf{V}_b^{\Delta x}) = \mathbb{F}^*(\mathbf{V}_a^{\Delta x}, \mathbf{V}_b^{\Delta x}) - \frac{1}{2} \mathbb{D}(\mathbf{V}_a^{\Delta x}, \mathbf{V}_b^{\Delta x})(\mathbf{V}_b^{\Delta x} - \mathbf{V}_a^{\Delta x}) \tag{5}$$

with

$$\mathbb{D}(\mathbf{a}, \mathbf{b}) = \mathbf{R} \, \mathbf{P}(\mathbf{\Lambda}; \mathbf{a}, \mathbf{b}) \, \mathbf{R}^T.$$

Here $\mathbf{\Lambda}$, $\mathbf{R}$ are the (real) eigenvalue and eigenvector matrices of the Jacobian $\partial_\mathbf{U} \mathbf{F}$. In this work, we use the Rusanov diffusion operator given by

$$\mathbf{P}(\mathbf{\Lambda}; \mathbf{a}, \mathbf{b}) = \max\left\{ \lambda_{\max}(\mathbf{a}), \lambda_{\max}(\mathbf{b}) \right\} \mathbf{I}_m$$

with $\lambda_{\max}(\mathbf{U})$ denoting the maximum wave speed. Several other choices are possible, see [26, 8, 9, 17]. In the following we will refer by $\mathbb{F}$ both to entropy stable and entropy conservative fluxes.

In the simplest form of the scheme, the discrete numerical solution $\mathbf{V}^{\Delta x} \in \mathcal{V}^k$ to (2) is then found as the solution of the system

$$\mathcal{B}_{\mathrm{DG}}(\mathbf{V}^{\Delta x}, \mathbf{\Phi}^{\Delta x}) = 0 \quad \forall \mathbf{\Phi}^{\Delta x} \in \mathcal{V}^k. \tag{6}$$

For problems involving shocks or discontinuities, however, this scheme exhibits oscillations and overshoot. Therefore, in the scheme developed in [17], streamline diffusion and shock capturing operators in the form of quasilinear forms $\mathcal{B}_{\mathrm{SD}}$ and $\mathcal{B}_{\mathrm{SC}}$ are added. We refer to the original method for details concerning these operators. Then, the discrete solution $\mathbf{V}^{\Delta x} \in \mathcal{V}^k$ is found as the solution to the system

$$\mathcal{B}(\mathbf{V}^{\Delta x}, \mathbf{\Phi}^{\Delta x}) = \mathcal{B}_{\mathrm{DG}}(\mathbf{V}^{\Delta x}, \mathbf{\Phi}^{\Delta x}) + \mathcal{B}_{\mathrm{SD}}(\mathbf{V}^{\Delta x}, \mathbf{\Phi}^{\Delta x}) + \mathcal{B}_{\mathrm{SC}}(\mathbf{V}^{\Delta x}, \mathbf{\Phi}^{\Delta x}) = 0 \tag{7}$$

for all $\mathbf{\Phi}^{\Delta x} \in \mathcal{V}^k$.

Remark 2.1. *In our extension of the original scheme from conservation laws to convection-diffusion systems, we do not use the streamline diffusion and shock capturing operators $\mathcal{B}_{\mathrm{SD}}$ and $\mathcal{B}_{\mathrm{SC}}$. Instead we base our extension on the system (6). We expect the natural viscosity introduced by the additional diffusion term to take over the role of the streamline diffusion and shock capturing operators in terms of avoiding overshoot. Numerical tests show that this is the case if the grid size is chosen fine enough to resolve the additional viscosity in the system.*

Among other properties, one can show that the method described in (7) (as well as the method in (6)) results in entropy stable discrete solutions.

Theorem 2.1 (Part of Theorem 3.1. in [17])**.** *Consider the system of conservation laws (1) with strictly convex entropy function S and entropy flux function Q. For simplicity, assume*

that the exact and approximate solutions have compact support inside the spatial domain Ω. Let the final time be denoted by t_-^N. Then the approximate solutions produced by (7) satisfy

$$\int_\Omega S(\mathbf{U}(\mathbf{V}^{\Delta x}(x, t_-^N)))\, dx \le \int_\Omega S(\mathbf{U}(\mathbf{V}^{\Delta x}(x, t_-^0)))\, dx.$$

This concludes our summary of the method for hyperbolic conservation laws and of the features that are relevant for our new methods. We will present the details of our extensions ST-IP-DG and ST-LDG in Sections 4 and 5. First, however, we will examine the effect of switching to entropy variables on the convection-diffusion systems that we consider.

3. Convection-diffusion systems written in entropy variables

We consider a system of conservation laws

$$\mathbf{U}_t + \mathbf{F}(\mathbf{U})_x = 0$$

and add a diffusion matrix $\mathbf{D} : \mathbb{R}^m \to \mathbb{R}^m$, to be thought of as, e.g., physical viscosity and heat conduction terms resulting in

$$\mathbf{U}_t + \mathbf{F}(\mathbf{U})_x = (\mathbf{D}(\mathbf{U})\mathbf{U}_x)_x.$$

We assume that we are given a strictly convex entropy function S with corresponding entropy flux Q. Using entropy variables $\mathbf{V} = S_\mathbf{U}(\mathbf{U})$ as degrees of freedom results in

$$\mathbf{U}(\mathbf{V})_t + \mathbf{F}(\mathbf{V})_x = (\mathbf{A}(\mathbf{V})\mathbf{V}_x)_x \tag{8}$$

with $\mathbf{A}(\mathbf{V}) = \mathbf{D}(\mathbf{U}(\mathbf{V}))\mathbf{U}_\mathbf{V}(\mathbf{V})$. It is well-known that such a change to entropy variables symmetrizes a hyperbolic system of conservation laws [11, 10, 20, 13]. Additionally, this change of variable can have a positive effect on the properties of the matrix $\mathbf{A}$.

3.1. The compressible Navier-Stokes equations

In this section we shortly describe the situation for the compressible Navier-Stokes equations, our main application. We focus on introducing the entropy S that we use and on discussing the properties of $\mathbf{A}$. Further information for using compressible Navier-Stokes equations with entropy variables can be found in the literature [12, 18, 25, 27].

The compressible Navier-Stokes equations in one space dimension are given by

$$\begin{aligned}
\rho_t + (\rho u)_x &= 0, \\
(\rho u)_t + (\rho u^2 + p)_x &= \nu u_{xx}, \\
E_t + ((E + p)u)_x &= \nu \left(\frac{u^2}{2}\right)_{xx} + \kappa\theta_{xx},
\end{aligned} \tag{9}$$

with $\rho = \rho(x, t)$ denoting the density, $u = u(x, t)$ the velocity, $p = p(x, t)$ the pressure, and $E = \frac{p}{\gamma-1} + \frac{1}{2}\rho u^2$ being the total energy. We will also use $m = m(x, t) = \rho(x, t)u(x, t)$ for the momentum. Additionally, $\theta = \frac{p}{R\rho}$ refers to the temperature. We assume the viscosity ν and

the conductivity κ to be constant. We further assume the relation between ν and κ/R to be given by the Prandtl number $P_r = 4\gamma/(9\gamma - 5)$ via

$$\frac{\kappa}{R} = \frac{\gamma C_v}{RP_r}\nu = \frac{9\gamma - 5}{4(\gamma - 1)}\nu.$$

Writing the right hand side of (9) in the form $(\mathbf{D}(\mathbf{U})\mathbf{U}_x)_x$ with $\mathbf{U} = (\rho, m, E)^T$ results in

$$\mathbf{D}(\mathbf{U}) = \begin{pmatrix} 0 & 0 & 0 \\ -\nu\frac{m}{\rho^2} & \frac{\nu}{\rho} & 0 \\ -\nu\frac{m^2}{\rho^3} + \frac{\kappa}{R}(\gamma - 1)\left(\frac{m^2}{\rho^3} - \frac{E}{\rho^2}\right) & \nu\frac{m}{\rho^2} - \frac{\kappa}{R}(\gamma - 1)\frac{m}{\rho^2} & \frac{\kappa}{R}\frac{\gamma-1}{\rho} \end{pmatrix}.$$

We note that the matrix $\mathbf{D}(\mathbf{U})$ is not symmetric.

For the transformation to entropy variables, we use the physical entropy and the corresponding entropy flux given by

$$S = \frac{-\rho s}{\gamma - 1}, \quad Q = \frac{-\rho u s}{\gamma - 1}, \quad s = \log(p) - \gamma\log(\rho).$$

This results in the entropy variables (written in terms of primitive variables and s for simplicity)

$$\mathbf{V} = \left(\frac{\gamma - s}{\gamma - 1} - \frac{\rho u^2}{2p}, \quad \frac{\rho u}{p}, \quad -\frac{\rho}{p}\right)^T.$$

The matrix $\mathbf{A}(\mathbf{V})$ is then given by

$$\mathbf{A}(\mathbf{V}) = \begin{pmatrix} 0 & 0 & 0 \\ 0 & -\nu\frac{1}{v_3} & \nu\frac{v_2}{v_3^2} \\ 0 & \nu\frac{v_2}{v_3^2} & -\nu\frac{v_2^2}{v_3^3} + \frac{\kappa}{R}\frac{1}{v_3^2} \end{pmatrix}. \tag{10}$$

For $\rho, p > 0$, this matrix is symmetric positive semi-definite. Furthermore, the reduced matrix

$$\tilde{\mathbf{A}}(\mathbf{V}) = \begin{pmatrix} -\nu\frac{1}{v_3} & \nu\frac{v_2}{v_3^2} \\ \nu\frac{v_2}{v_3^2} & -\nu\frac{v_2^2}{v_3^3} + \frac{\kappa}{R}\frac{1}{v_3^2} \end{pmatrix} \tag{11}$$

is symmetric positive definite with eigenvalues

$$\lambda_{1,2} = \frac{1}{2}\left(-b \mp \sqrt{b^2 + 4\nu\frac{\kappa}{R}\frac{1}{v_3^3}}\right) > 0, \quad b = \nu\frac{v_2^2}{v_3^3} - \frac{\kappa}{R}\frac{1}{v_3^2} + \frac{\nu}{v_3}, \tag{12}$$

if $\nu, \kappa > 0$ and $\rho, p > 0$.

4. The ST-IP-DG method

In this section, we present our extension that is based on the IP approach by Arnold [1] as well as on earlier work by Nitsche [21]. For simplicity, we focus on the description of the scheme in the interior of the domain. Necessary modifications for boundary edges will be discussed in Appendix A.

In the ST-IP-DG method, in order to numerically solve the system (8) with homogeneous Dirichlet boundary conditions, we solve the quasilinear form

$$\mathcal{B}_{\mathrm{DG}}(\mathbf{V}^{\Delta x}, \boldsymbol{\Phi}^{\Delta x}) + \mathcal{B}_{\mathrm{IP}}(\mathbf{V}^{\Delta x}, \boldsymbol{\Phi}^{\Delta x}) = 0 \quad \forall \, \boldsymbol{\Phi}^{\Delta x} \in \mathcal{V}^k. \tag{13}$$

Here, $\mathcal{B}_{\mathrm{IP}}(\mathbf{V}^{\Delta x}, \boldsymbol{\Phi}^{\Delta x})$ represents the IP-discretization of the diffusion term $(\mathbf{A}(\mathbf{V})\mathbf{V}_x)_x$ and is given by

$$
\begin{aligned}
\mathcal{B}_{\mathrm{IP}}(\mathbf{V}^{\Delta x}, \boldsymbol{\Phi}^{\Delta x}) = &\sum_{n,i} \int_{I_n} \int_{K_i} \langle \mathbf{A}(\mathbf{V}^{\Delta x}) \mathbf{V}_x^{\Delta x}, \boldsymbol{\Phi}_x^{\Delta x} \rangle \, dx \, dt \\
&+ \sum_{n,i} \int_{I_n} \langle \mathbf{A}(\{\mathbf{V}^{\Delta x}\}) \{\mathbf{V}_x^{\Delta x}\}_{i+1/2}, [\boldsymbol{\Phi}^{\Delta x}]_{i+1/2} \rangle \, dt \\
&+ \sum_{n,i} \int_{I_n} \langle \mathbf{A}(\{\mathbf{V}^{\Delta x}\})[\mathbf{V}^{\Delta x}]_{i+1/2}, \{\boldsymbol{\Phi}_x^{\Delta x}\}_{i+1/2} \rangle \, dt \\
&+ \sum_{n,i} \int_{I_n} \frac{\gamma}{\Delta x} \langle \mathbf{A}(\{\mathbf{V}^{\Delta x}\})[\mathbf{V}^{\Delta x}]_{i+1/2}, [\boldsymbol{\Phi}^{\Delta x}]_{i+1/2} \rangle \, dt
\end{aligned} \tag{14}
$$

for interior edges $i \pm 1/2$. We use the standard notation for average and jump given by

$$\{v^{\Delta x}\}_{i+1/2} = \frac{1}{2}\left(v_{i+1/2,R}^{\Delta x} + v_{i+1/2,L}^{\Delta x}\right), \quad [v^{\Delta x}]_{i+1/2} = v_{i+1/2,R}^{\Delta x} - v_{i+1/2,L}^{\Delta x}.$$

We note that the edge terms in the second line result from integration by parts using central fluxes. The edge terms in the third line are added to make the form symmetric. Finally, the jump terms in the fourth line are stabilization terms that enforce coercivity of the form $\mathcal{B}_{\mathrm{IP}}$ with the parameter γ being the penalty parameter.

In order to show entropy stability of the described method, we need to make the following assumption.

Assumption 4.1. *We assume that the matrix $\mathbf{A}(\mathbf{V}) : \mathbb{R}^m \to \mathbb{R}^m$ in (8) is symmetric positive definite. We further assume that there are lower and upper bounds (λ, Λ) on the eigenvalues of $\mathbf{A}$ such that $0 < \lambda \leq \lambda_1 \leq \lambda_2 \leq \ldots \leq \lambda_m \leq \Lambda$.*

Then, we can show the following statement.

Theorem 4.1. *Consider the system (8) and let Assumption 4.1 hold true. Further assume that S is strictly convex. For simplicity, also assume that the exact and approximate solutions have compact support inside the spatial domain. Let the final time be denoted by t_-^N. Then, the approximate solutions generated by the scheme (13) satisfy*

$$\int_\Omega S(\mathbf{U}(\mathbf{V}^{\Delta x}(x, t_-^N))) \, dx \leq \int_\Omega S(\mathbf{U}(\mathbf{V}^{\Delta x}(x, t_-^0))) \, dx,$$

provided γ is chosen sufficiently large such that

$$\min\left(\lambda - c_{\mathrm{inv}} \delta \Lambda, \gamma - \frac{1}{\delta}\right) > 0, \tag{15}$$

where λ, Λ are defined in Assumption 4.1, c_{inv} will be specified later in Lemma 4.2, and $\delta > 0$ can be chosen freely to balance both conditions.

To prove the theorem, we will need the following lemma, which generalizes Young's inequality to matrices.

Lemma 4.1. *Let the matrix $\mathbf{C} : \mathbb{R}^m \to \mathbb{R}^m$ be symmetric positive definite. Then there holds for arbitrary vectors $v, w \in \mathbb{R}^m$ and $\delta > 0$*

$$2w^T \mathbf{C} v \leq \delta w^T \mathbf{C} w + \frac{1}{\delta} v^T \mathbf{C} v.$$

We also need the following inverse estimate.

Lemma 4.2. *For the discrete spacetime polynomials there holds*

$$\int_{I^n} (v_{x,B}^{\Delta x})^2 \, dt \leq \frac{c_{\mathrm{inv}}}{\Delta x} \int_{I^n} \int_{K_i} (v_x^{\Delta x})^2 \, dx \, dt$$

with $v_{x,B}^{\Delta x} = v_{x,i+1/2,L}^{\Delta x}$ or $v_{x,B}^{\Delta x} = v_{x,i-1/2,R}^{\Delta x}$.

With these prerequisites, we can prove Theorem 4.1.

Proof of Theorem 4.1. We set $\mathbf{\Phi}^{\Delta x} = \mathbf{V}^{\Delta x}$ resulting in

$$\mathcal{B}_{\mathrm{DG}}(\mathbf{V}^{\Delta x}, \mathbf{V}^{\Delta x}) + \mathcal{B}_{\mathrm{IP}}(\mathbf{V}^{\Delta x}, \mathbf{V}^{\Delta x}) = 0.$$

The proof consists of two parts: in **Part 1**, we show

$$\mathcal{B}_{\mathrm{DG}}(\mathbf{V}^{\Delta x}, \mathbf{V}^{\Delta x}) \geq \int_{\Omega} S(\mathbf{U}(\mathbf{V}^{\Delta x}(x, t_-^N))) \, dx - \int_{\Omega} S(\mathbf{U}(\mathbf{V}^{\Delta x}(x, t_-^0))) \, dx. \tag{16}$$

In **Part 2**, we show that for γ sufficiently large, there holds $\mathcal{B}_{\mathrm{IP}}(\mathbf{V}^{\Delta x}, \mathbf{V}^{\Delta x}) \geq 0$. The two parts together imply the claim.

Part 1: The proof of (16) can be transferred from the proof of the entropy stability of the original scheme. Therefore, we do not give all details here. The full proof can be found in [17, Thm 3.1].

Step 1: Define the spatial part

$$\mathcal{B}_{\mathrm{DG}}^s(\mathbf{V}^{\Delta x}, \mathbf{\Phi}^{\Delta x}) = -\sum_{n,i} \int_{I^n} \int_{K_i} \langle \mathbf{F}(\mathbf{V}^{\Delta x}), \mathbf{\Phi}_x^{\Delta x} \rangle \, dx \, dt$$

$$+ \sum_{n,i} \int_{I^n} \left(\langle \mathbb{F}(\mathbf{V}_{i+1/2,L}^{\Delta x}, \mathbf{V}_{i+1/2,R}^{\Delta x}), \mathbf{\Phi}_{i+1/2,L}^{\Delta x} \rangle - \langle \mathbb{F}(\mathbf{V}_{i-1/2,L}^{\Delta x}, \mathbf{V}_{i-1/2,R}^{\Delta x}), \mathbf{\Phi}_{i-1/2,R}^{\Delta x} \rangle \right) \, dt.$$

One can show that $\mathcal{B}_{\mathrm{DG}}^s(\mathbf{V}^{\Delta x}, \mathbf{V}^{\Delta x}) \geq 0$: Due to the definition of the entropy flux function Q, there holds for the entropy potential $\psi_x = \langle \mathbf{V}_x, \mathbf{F} \rangle$. This implies

$$\mathcal{B}_{\mathrm{DG}}^s(\mathbf{V}^{\Delta x}, \mathbf{V}^{\Delta x}) = -\sum_{n,i} \int_{I^n} \int_{K_i} \psi(\mathbf{V}^{\Delta x})_x \, dx \, dt$$

$$+ \sum_{n,i} \int_{I^n} \left(\langle \mathbb{F}(\mathbf{V}_{i+1/2,L}^{\Delta x}, \mathbf{V}_{i+1/2,R}^{\Delta x}), \mathbf{V}_{i+1/2,L}^{\Delta x} \rangle - \langle \mathbb{F}(\mathbf{V}_{i-1/2,L}^{\Delta x}, \mathbf{V}_{i-1/2,R}^{\Delta x}), \mathbf{V}_{i-1/2,R}^{\Delta x} \rangle \right) \, dt.$$

8

Evaluating the (spatial) integral over ψ_x and using the definition of the flux $\mathbb{F}$ from (5) give

$$\mathcal{B}_{\mathrm{DG}}^s(\mathbf{V}^{\Delta x}, \mathbf{V}^{\Delta x}) = \sum_{n,i} \int_{I^n} \left(\langle \mathbb{F}^*(\mathbf{V}_{i+1/2,L}^{\Delta x}, \mathbf{V}_{i+1/2,R}^{\Delta x}), \mathbf{V}_{i+1/2,L}^{\Delta x} \rangle - \psi(\mathbf{V}_{i+1/2,L}^{\Delta x}) \right) dt$$

$$- \sum_{n,i} \int_{I^n} \left(\langle \mathbb{F}^*(\mathbf{V}_{i-1/2,L}^{\Delta x}, \mathbf{V}_{i-1/2,R}^{\Delta x}), \mathbf{V}_{i-1/2,R}^{\Delta x} \rangle - \psi(\mathbf{V}_{i-1/2,R}^{\Delta x}) \right) dt$$

$$- \frac{1}{2} \sum_{n,i} \int_{I^n} \langle \mathbf{V}_{i+1/2,L}^{\Delta x}, \mathbb{D}(\mathbf{V}_{i+1/2,R}^{\Delta x} - \mathbf{V}_{i+1/2,L}^{\Delta x}) \rangle \, dt$$

$$+ \frac{1}{2} \sum_{n,i} \int_{I^n} \langle \mathbf{V}_{i-1/2,R}^{\Delta x}, \mathbb{D}(\mathbf{V}_{i-1/2,R}^{\Delta x} - \mathbf{V}_{i-1/2,L}^{\Delta x}) \rangle \, dt.$$

Reordering the sum and exploiting the compact support of the approximate solutions result in

$$\mathcal{B}_{\mathrm{DG}}^s(\mathbf{V}^{\Delta x}, \mathbf{V}^{\Delta x}) = -\sum_{n,i} \int_{I^n} \big(\langle \mathbb{F}^*(\mathbf{V}_{i+1/2,L}^{\Delta x}, \mathbf{V}_{i+1/2,R}^{\Delta x}), \mathbf{V}_{i+1/2,R}^{\Delta x} - \mathbf{V}_{i+1/2,L}^{\Delta x} \rangle$$

$$- (\psi(\mathbf{V}_{i+1/2,R}^{\Delta x}) - \psi(\mathbf{V}_{i+1/2,L}^{\Delta x})) \big) \, dt$$

$$+ \frac{1}{2} \sum_{n,i} \int_{I^n} \langle \mathbf{V}_{i+1/2,R}^{\Delta x} - \mathbf{V}_{i+1/2,L}^{\Delta x}, \mathbb{D}(\mathbf{V}_{i+1/2,R}^{\Delta x} - \mathbf{V}_{i+1/2,L}^{\Delta x}) \rangle \, dt.$$

The terms in the first sum cancel due to (4), the terms in the second sum are non-negative due to the definition of the diffusion operator $\mathbb{D}$.

Step 2: Define the temporal part

$$\mathcal{B}_{\mathrm{DG}}^t(\mathbf{V}^{\Delta x}, \mathbf{\Phi}^{\Delta x}) = -\sum_{n,i} \int_{I^n} \int_{K_i} \langle \mathbf{U}(\mathbf{V}^{\Delta x}), \mathbf{\Phi}_t^{\Delta x} \rangle \, dx \, dt$$

$$+ \sum_{n,i} \int_{K_i} \left(\langle \mathbf{U}(\mathbf{V}_{n+1,-}^{\Delta x}), \mathbf{\Phi}_{n+1,-}^{\Delta x} \rangle - \langle \mathbf{U}(\mathbf{V}_{n,-}^{\Delta x}), \mathbf{\Phi}_{n,+}^{\Delta x} \rangle \right) \, dx.$$

Set $\mathbf{\Phi}^{\Delta x} = \mathbf{V}^{\Delta x}$ and use integration by parts with respect to time. The boundary terms evaluated at t_-^{n+1} cancel resulting in

$$\mathcal{B}_{\mathrm{DG}}^t(\mathbf{V}^{\Delta x}, \mathbf{V}^{\Delta x}) = \sum_{n,i} \int_{I^n} \int_{K_i} \langle \mathbf{U}(\mathbf{V}^{\Delta x})_t, \mathbf{V}^{\Delta x} \rangle \, dx \, dt$$

$$+ \sum_{n,i} \int_{K_i} \left(\langle \mathbf{U}(\mathbf{V}_{n,+}^{\Delta x}), \mathbf{V}_{n,+}^{\Delta x} \rangle - \langle \mathbf{U}(\mathbf{V}_{n,-}^{\Delta x}), \mathbf{V}_{n,+}^{\Delta x} \rangle \right) \, dx.$$

By the definition of the entropy function, $\langle \mathbf{U}(\mathbf{V}^{\Delta x})_t, \mathbf{V}^{\Delta x} \rangle = S(\mathbf{U}(\mathbf{V}^{\Delta x}))_t$. Evaluating the time integral and adding a zero-sum involving $S(\mathbf{U}(\mathbf{V}_{n,-}^{\Delta x}))$, this implies

$$\mathcal{B}_{\mathrm{DG}}^t(\mathbf{V}^{\Delta x}, \mathbf{V}^{\Delta x}) = \sum_{n,i} \int_{K_i} \left(S(\mathbf{U}(\mathbf{V}_{n+1,-}^{\Delta x})) - S(\mathbf{U}(\mathbf{V}_{n,-}^{\Delta x})) \right) \, dx$$

$$+ \sum_{n,i} \int_{K_i} \left(S(\mathbf{U}(\mathbf{V}_{n,-}^{\Delta x})) - S(\mathbf{U}(\mathbf{V}_{n,+}^{\Delta x})) \right) \, dx + \sum_{n,i} \int_{K_i} \langle \mathbf{U}(\mathbf{V}_{n,+}^{\Delta x}) - \mathbf{U}(\mathbf{V}_{n,-}^{\Delta x}), \mathbf{V}_{n,+}^{\Delta x} \rangle \, dx.$$

The first sum corresponds to a telescope sum. For the second and third sum, the change of variables $\mathbf{V}(\theta) = \theta\mathbf{V}_{n,-} + (1 - \theta)\mathbf{V}_{n,+}$ is used. This results in

$$\mathcal{B}_{\mathrm{DG}}^t(\mathbf{V}^{\Delta x}, \mathbf{V}^{\Delta x}) = \int_\Omega \left(S(\mathbf{U}(\mathbf{V}^{\Delta x}(x, t_-^N))) - S(\mathbf{U}(\mathbf{V}^{\Delta x}(x, t_-^0))) \right) \, dx$$

$$+ \sum_{n,i} \int_{K_i} \int_0^1 \theta \left\langle \mathbf{V}_{n,-} - \mathbf{V}_{n,+}, \mathbf{U}_\mathbf{V}(\theta)(\mathbf{V}_{n,-} - \mathbf{V}_{n,+}) \right\rangle d\theta \, dx.$$

Due to S being strictly convex, the terms in the second line are positive, implying

$$\mathcal{B}_{\mathrm{DG}}^t(\mathbf{V}^{\Delta x}, \mathbf{V}^{\Delta x}) \geq \int_\Omega S\left(\mathbf{U}(\mathbf{V}^{\Delta x}(x, t_-^N))\right) \, dx - \int_\Omega S\left(\mathbf{U}(\mathbf{V}^{\Delta x}(x, t_-^0))\right) \, dx.$$

This concludes the proof of **Part 1**.

Part 2: We now need to show $\mathcal{B}_{\mathrm{IP}}(\mathbf{V}^{\Delta x}, \mathbf{V}^{\Delta x}) \geq 0$. Due to the solutions having compact support, there holds

$$\mathcal{B}_{\mathrm{IP}}(\mathbf{V}^{\Delta x}, \mathbf{V}^{\Delta x}) = \sum_{n,i} \int_{I_n} \int_{K_i} \underbrace{\left\langle \mathbf{A}(\mathbf{V}^{\Delta x})\mathbf{V}_x^{\Delta x}, \mathbf{V}_x^{\Delta x} \right\rangle}_{\Gamma_1} \, dx \, dt$$

$$+ 2\sum_{n,i} \int_{I_n} \left\langle \mathbf{A}(\{\mathbf{V}^{\Delta x}\}) \left\{\mathbf{V}_x^{\Delta x}\right\}_{i+1/2}, [\mathbf{V}^{\Delta x}]_{i+1/2} \right\rangle \, dt$$

$$+ \sum_{n,i} \int_{I_n} \underbrace{\frac{\gamma}{\Delta x}\left\langle \mathbf{A}(\{\mathbf{V}^{\Delta x}\})[\mathbf{V}^{\Delta x}]_{i+1/2}, [\mathbf{V}^{\Delta x}]_{i+1/2} \right\rangle}_{\Gamma_2} \, dt.$$

Based on Assumption 4.1, the matrix $\mathbf{A}$ is positive definite. This implies that both Γ_1 and Γ_2 are positive unless $\mathbf{V}_x^{\Delta x} \equiv \mathbf{0}$ or $\mathbf{V}^{\Delta x}$ is continuous. Applying Lemma 4.1 with arbitrary $\delta > 0$ to the potentially negative term results in

$$2\langle \mathbf{A}(\{\mathbf{V}^{\Delta x}\}) \left\{\mathbf{V}_x^{\Delta x}\right\}_{i+1/2}, [\mathbf{V}^{\Delta x}]_{i+1/2}\rangle$$

$$\leq \underbrace{\delta\Delta x\langle \mathbf{A}(\{\mathbf{V}^{\Delta x}\}) \left\{\mathbf{V}_x^{\Delta x}\right\}_{i+1/2}, \left\{\mathbf{V}_x^{\Delta x}\right\}_{i+1/2}\rangle}_{\Pi_1} + \underbrace{\frac{1}{\delta\Delta x}\langle \mathbf{A}(\{\mathbf{V}^{\Delta x}\})[\mathbf{V}^{\Delta x}]_{i+1/2}, [\mathbf{V}^{\Delta x}]_{i+1/2}\rangle}_{\Pi_2}.$$

Choosing $\gamma > \frac{1}{\delta}$, the term Π_2 can be compensated by Γ_2

$$-\sum_{n,i} \int_{I_n} \Pi_2 \, dt + \sum_{n,i} \int_{I_n} \Gamma_2 \, dt = \frac{\gamma - \frac{1}{\delta}}{\Delta x} \sum_{n,i} \int_{I_n} \langle \mathbf{A}(\{\mathbf{V}^{\Delta x}\})[\mathbf{V}^{\Delta x}]_{i+1/2}, [\mathbf{V}^{\Delta x}]_{i+1/2}\rangle \, dt.$$

In the following we determine a value δ_0 such that for $\delta \leq \delta_0$ the term Γ_1 dominates the term Π_1. Then choosing $\gamma > 1/\delta_0$ implies the claim. By assumption, the eigenvalues of the matrix $\mathbf{A}$ are uniformly bounded in the following way

$$0 < \lambda \leq \lambda_1 \leq \ldots \leq \lambda_m \leq \Lambda.$$

This implies

$$\sum_{n,i} \int_{I_n} \int_{K_i} \Gamma_1 \, dx \, dt - \sum_{n,i} \int_{I_n} \Pi_1 \, dt \geq$$

$$\sum_{n,i} \int_{I_n} \int_{K_i} \lambda\langle \mathbf{V}_x^{\Delta x}, \mathbf{V}_x^{\Delta x}\rangle \, dx \, dt - \sum_{n,i} \int_{I_n} \delta\Delta x\Lambda\langle \left\{\mathbf{V}_x^{\Delta x}\right\}_{i+1/2}, \left\{\mathbf{V}_x^{\Delta x}\right\}_{i+1/2}\rangle \, dt.$$

10

As

$$\langle\{\mathbf{V}_x^{\Delta x}\}_{i+1/2}, \{\mathbf{V}_x^{\Delta x}\}_{i+1/2}\rangle = \sum_{j=1}^{m}\left(\{(v_j^{\Delta x})_x\}_{i+1/2}\right)^2,$$

we can apply an inverse estimate to each component. Using

$$\left(\{v_x^{\Delta x}\}_{i+1/2}\right)^2 = \left(\frac{1}{2}(v_{x,i+1/2,L}^{\Delta x} + v_{x,i+1/2,R}^{\Delta x})\right)^2 \leq \frac{1}{2}(v_{x,i+1/2,L}^{\Delta x})^2 + \frac{1}{2}(v_{x,i+1/2,R}^{\Delta x})^2$$

and Lemma 4.2, we get

$$\sum_{n,i}\int_{I_n}\delta\Delta x\Lambda\langle\{\mathbf{V}_x^{\Delta x}\}_{i+1/2}, \{\mathbf{V}_x^{\Delta x}\}_{i+1/2}\rangle \, dt \leq \sum_{n,i}\int_{I_n}\int_{K_i}c_{\mathrm{inv}}\delta\Lambda\langle\mathbf{V}_x^{\Delta x}, \mathbf{V}_x^{\Delta x}\rangle \, dx \, dt.$$

This implies

$$\sum_{n,i}\int_{I_n}\int_{K_i}\Gamma_1 \, dx \, dt - \sum_{n,i}\int_{I_n}\Pi_1 \, dt \geq (\lambda - c_{\mathrm{inv}}\delta\Lambda)\sum_{n,i}\int_{I_n}\int_{K_i}\langle\mathbf{V}_x^{\Delta x}, \mathbf{V}_x^{\Delta x}\rangle \, dx \, dt.$$

Summarizing all results, there holds

$$\mathcal{B}_{\mathrm{IP}}(\mathbf{V}^{\Delta x}, \mathbf{V}^{\Delta x}) \geq (\lambda - c_{\mathrm{inv}}\delta\Lambda)\sum_{n,i}\int_{I_n}\int_{K_i}\langle\mathbf{V}_x^{\Delta x}, \mathbf{V}_x^{\Delta x}\rangle \, dx \, dt$$
$$+ \frac{\gamma - \frac{1}{\delta}}{h}\sum_{n,i}\int_{I_n}\langle\mathbf{A}(\{\mathbf{V}^{\Delta x}\})[\mathbf{V}^{\Delta x}]_{i+1/2}, [\mathbf{V}^{\Delta x}]_{i+1/2}\rangle \, dt,$$

which implies the claim. $\qquad\square$

Remark 4.1. *1. We note that only the parameter γ appears in the actual method. The parameter δ only exists for theoretical considerations.*

2. For solving the scalar equation $u_t + f(u)_x = (au_x)_x$ with $0 < \underline{a} \leq a \leq \overline{a}$ and bounds $m \leq S_{uu} \leq M$ the condition (15) on γ reduces to

$$\min\left(\frac{\underline{a}}{M} - \frac{\overline{a}\,\delta\,c_{\mathrm{inv}}}{m}, \gamma - \frac{1}{\delta}\right) > 0. \tag{17}$$

3. When using a non-symmetric IP (NIPG) approach, compare [24], the sum in the third line of the definition of $\mathcal{B}_{\mathrm{IP}}$ in (14) has a negative sign. Therefore, the possibly negative terms

$$\langle\mathbf{A}(\{\mathbf{V}^{\Delta x}\})\{\mathbf{V}_x^{\Delta x}\}_{i+1/2}, [\mathbf{\Phi}^{\Delta x}]_{i+1/2}\rangle \;\; \text{and} \;\; \langle\mathbf{A}(\{\mathbf{V}^{\Delta x}\})[\mathbf{V}^{\Delta x}]_{i+1/2}, \{\mathbf{\Phi}_x^{\Delta x}\}_{i+1/2}\rangle$$

cancel each other in the stability estimate. As a result, the method is stable for any value $\gamma \geq 0$. However, the NIPG method is known to lead to a decay in convergence order. We also observed this decay for even polynomial degrees in our tests. Therefore, we currently prefer the symmetric version of the IP method but might consider the NIPG version for our extension to higher space dimensions due to its better stability properties.

4.1. The ST-IP-DG method applied to the compressible Navier-Stokes equations

We now examine in how far Assumption 4.1, which is needed for proving entropy stability of the ST-IP-DG method, is satisfied for our main application, the compressible Navier-Stokes equations.

As noted in Section 3.1, the matrix $\mathbf{A}$ corresponding to the compressible Navier-Stokes equations with our choice of entropy variables is symmetric positive semi-definite, not positive definite. However, $\mathbf{A}$ has the structure

$$\mathbf{A} = \begin{bmatrix} 0 & 0 \\ 0 & \tilde{\mathbf{A}} \end{bmatrix}.$$

Therefore, defining $\tilde{\mathbf{V}}^{\Delta x} = (v_2^{\Delta x}, v_3^{\Delta x})$ and $\tilde{\boldsymbol{\Phi}}^{\Delta x} = (\Phi_2^{\Delta x}, \Phi_3^{\Delta x})$, there holds

$$\mathcal{B}_{\mathrm{IP}}(\mathbf{V}^{\Delta x}, \boldsymbol{\Phi}^{\Delta x}) = \widetilde{\mathcal{B}_{\mathrm{IP}}}(\tilde{\mathbf{V}}^{\Delta x}, \tilde{\boldsymbol{\Phi}}^{\Delta x}) \quad \forall\, \mathbf{V}^{\Delta x}, \boldsymbol{\Phi}^{\Delta x} \in \mathcal{V}^k,$$

with $\widetilde{\mathcal{B}_{\mathrm{IP}}}$ defined as $\mathcal{B}_{\mathrm{IP}}$ (compare (14)) but with $\mathbf{A}$ replaced by $\tilde{\mathbf{A}}$ and the scalar product being taken only over 2 components. Due to this equivalence, it is sufficient to implement the shortened form $\widetilde{\mathcal{B}_{\mathrm{IP}}}$. For entropy stability, one now needs to show

$$\widetilde{\mathcal{B}_{\mathrm{IP}}}(\tilde{\mathbf{V}}^{\Delta x}, \tilde{\mathbf{V}}^{\Delta x}) \geq 0.$$

In order to apply the proof of Theorem 4.1, Assumption 4.1 needs to be satisfied for the matrix $\tilde{\mathbf{A}}$. As discussed in Section 3.1, the matrix $\tilde{\mathbf{A}}$ is symmetric positive definite. Additionally, one needs to show uniform bounds λ, Λ on the eigenvalues of $\tilde{\mathbf{A}}$ given by (12). We do not know of general, problem-independent uniform bounds of this form. However, under the following assumptions, one can deduce such bounds and therefore satisfy all assumptions made in Assumption 4.1. Then, the proof of entropy stability is applicable to the compressible Navier-Stokes equations.

Assumption 4.2. *We assume that there are uniform lower bounds $\rho_0, p_0 > 0$ such that $\rho \geq \rho_0$ and $p \geq p_0$. We further assume that there are uniform upper bounds $\rho_M, u_M, p_M > 0$ such that $\rho \leq \rho_M$, $|u| \leq u_M$, and $p \leq p_M$.*

Lemma 4.3. *Under Assumption 4.2, there exist $\lambda(\rho_M, u_M, p_0)$ and $\Lambda(\rho_0, u_M, p_M)$ such that $0 < \lambda \leq \lambda_1 < \lambda_2 \leq \Lambda$ for the eigenvalues of $\tilde{\mathbf{A}}$.*

Proof. The eigenvalues $\lambda_{1,2}$ of $\tilde{\mathbf{A}}$ are given by (12) with λ_2 corresponding to the '+' sign. We can bound λ_2 from above by $\lambda_2 \leq |b|$. Then, we can bound $|b|$ using Assumption 4.2 in terms of ρ_0, u_M, and p_M. For the lower bound, we write

$$\lambda_1 = \frac{1}{2}|b|\left(1 - \sqrt{1-\varepsilon}\right), \quad \varepsilon = -\frac{4\nu\frac{\kappa}{R}\frac{1}{v_3^3}}{b^2}.$$

We note that $0 < \varepsilon < 1$. We use the Taylor expansion of the square root function to bound

$$\sqrt{1-\varepsilon} \leq 1 - \frac{1}{2}\varepsilon.$$

This implies $\lambda_1 \geq \frac{1}{4}|b|\,\varepsilon$, which in turn can be bounded using Assumption 4.2 in terms of ρ_M, u_M, and p_0. $\square$

5. The ST-LDG method

Our second approach for extending the original spacetime DG method is a variant of the LDG method introduced by Cockburn and Shu [7]. We will shortly describe the situation for scalar equations in order to motivate why just following the original LDG method does not do the trick. Then we will describe our new ST-LDG method for convection-diffusion systems.

5.1. Motivation: The situation for scalar equations

Let us consider the scalar equation $u(v)_t + f(v)_x = (au_v(v)v_x)_x$, already expressed in entropy variables. We introduce the auxiliary variable

$$p = \sqrt{au_v(v)}v_x$$

and rewrite the original equation as a system of two first-order equations,

$$u(v)_t + f(v)_x = (\sqrt{au_v(v)}p)_x,$$
$$p - g(v)_x = 0,$$

with the auxiliary function

$$g(v) = \int^v \sqrt{au_v(s)}ds.$$

The function g has been introduced to write the system in conservation form. For a spacetime DG approach this formulation requires to evaluate jumps and averages of g at cell edges as well as spacetime integrals over g. While this is trivial for a and u_v being constant, and one can easily modify the method to result in an entropy stable spacetime DG method, this is not the case for the systems that we are interested in: here, $\mathbf{U_V}(\mathbf{V})$ is typically a non-constant matrix depending non-linearly on $\mathbf{V}$. Therefore, our ST-LDG method uses a non-conservative formulation in the equation for the auxiliary variable.

5.2. The ST-LDG method

We consider the convection-diffusion system

$$\mathbf{U}(\mathbf{V})_t + \mathbf{F}(\mathbf{V})_x = (\mathbf{A}(\mathbf{V})\mathbf{V}_x)_x.$$

In order to define the ST-LDG method for systems, we need to make the following assumption.

Assumption 5.1. *We assume that the matrix $\mathbf{A}(\mathbf{V}) : \mathbb{R}^m \to \mathbb{R}^m$ in (8) is symmetric positive semi-definite.*

Assumption 5.1 implies that there exists a symmetric positive semi-definite matrix $\mathbf{B}(\mathbf{V})$ such that $\mathbf{B}^2 = \mathbf{A}$.

Remark 5.1. *We note that Assumption 5.1 is satisfied for the compressible Navier-Stokes equations with our choice of entropy variables as discussed in Section 3.1. We will describe the matrix $\mathbf{B}$ that we use in our numerical algorithm in Appendix B.*

Therefore, the system above is equivalent to

$$\mathbf{U}_t + \mathbf{F}(\mathbf{U}(\mathbf{V}))_x = (\mathbf{B}^2(\mathbf{V})\mathbf{V}_x)_x.$$

We define $\mathbf{P} = \mathbf{B}(\mathbf{V})\mathbf{V}_x$ and rewrite the second-order system as

$$\mathbf{U}_t + \mathbf{F}(\mathbf{U}(\mathbf{V}))_x = (\mathbf{B}(\mathbf{V})\mathbf{P})_x,$$
$$\mathbf{P} = \mathbf{B}(\mathbf{V})\mathbf{V}_x.$$

We note that the first set of equations, which contains the conserved quantity $\mathbf{U}$, is written in conservation form, while the second set of equations uses a non-conservative formulation.

Let the discrete solution be given by the pair $\mathbf{W}^{\Delta x} = (\mathbf{V}^{\Delta x}, \mathbf{P}^{\Delta x})$. To deduce the variational formulation, we multiply the first set of equations with a test function $\mathbf{\Phi}^{\Delta x}$, integrate over spacetime elements, and do integration by parts using central fluxes for the diffusion terms. This results in

$$
\begin{aligned}
\mathcal{B}^1(\mathbf{W}^{\Delta x}, \mathbf{\Phi}^{\Delta x}) = {}& \mathcal{B}_{\mathrm{DG}}(\mathbf{V}^{\Delta x}, \mathbf{\Phi}^{\Delta x}) \\
& + \sum_{n,i} \int_{I^n} \int_{K_i} \langle \mathbf{B}(\mathbf{V}^{\Delta x})\mathbf{P}^{\Delta x}, \mathbf{\Phi}_x^{\Delta x} \rangle \, dx \, dt \\
& - \sum_{n,i} \int_{I^n} \left\langle \frac{\mathbf{B}(\mathbf{V}_{i+1/2,L}^{\Delta x}) + \mathbf{B}(\mathbf{V}_{i+1/2,R}^{\Delta x})}{2} \{\mathbf{P}^{\Delta x}\}_{i+1/2}, \mathbf{\Phi}_{i+1/2,L}^{\Delta x} \right\rangle \, dt \\
& + \sum_{n,i} \int_{I^n} \left\langle \frac{\mathbf{B}(\mathbf{V}_{i-1/2,L}^{\Delta x}) + \mathbf{B}(\mathbf{V}_{i-1/2,R}^{\Delta x})}{2} \{\mathbf{P}^{\Delta x}\}_{i-1/2}, \mathbf{\Phi}_{i-1/2,R}^{\Delta x} \right\rangle \, dt.
\end{aligned}
\tag{18}
$$

For the discretization of the non-conservative equations $\mathbf{P} = \mathbf{B}(\mathbf{V})\mathbf{V}_x$, we multiply both sides with a test function $\mathbf{\Psi}^{\Delta x}$, integrate over spacetime elements, and then add stability terms resulting in

$$
\begin{aligned}
\mathcal{B}^2(\mathbf{W}^{\Delta x}, \mathbf{\Psi}^{\Delta x}) = {}& \sum_{n,i} \int_{I^n} \int_{K_i} \langle \mathbf{P}^{\Delta x}, \mathbf{\Psi}^{\Delta x} \rangle \, dx \, dt \\
& - \sum_{n,i} \int_{I^n} \int_{K_i} \langle \mathbf{B}(\mathbf{V}^{\Delta x})\mathbf{V}_x^{\Delta x}, \mathbf{\Psi}^{\Delta x} \rangle \, dx \, dt \\
& - \frac{1}{2} \sum_{n,i} \int_{I^n} \left\langle \frac{\mathbf{B}(\mathbf{V}_{i+1/2,L}^{\Delta x}) + \mathbf{B}(\mathbf{V}_{i+1/2,R}^{\Delta x})}{2} [\mathbf{V}^{\Delta x}]_{i+1/2}, \mathbf{\Psi}_{i+1/2,L}^{\Delta x} \right\rangle \, dt \\
& - \frac{1}{2} \sum_{n,i} \int_{I^n} \left\langle \frac{\mathbf{B}(\mathbf{V}_{i-1/2,L}^{\Delta x}) + \mathbf{B}(\mathbf{V}_{i-1/2,R}^{\Delta x})}{2} [\mathbf{V}^{\Delta x}]_{i-1/2}, \mathbf{\Psi}_{i-1/2,R}^{\Delta x} \right\rangle \, dt.
\end{aligned}
\tag{19}
$$

The method then reads: find $\mathbf{W}^{\Delta x} = (\mathbf{V}^{\Delta x}, \mathbf{P}^{\Delta x}) \in \mathcal{V}^k \times \mathcal{V}^k$ such that

$$\mathcal{B}_{\mathrm{ST-LDG}}(\mathbf{W}^{\Delta x}, \mathbf{\Sigma}^{\Delta x}) = \mathcal{B}^1(\mathbf{W}^{\Delta x}, \mathbf{\Phi}^{\Delta x}) + \mathcal{B}^2(\mathbf{W}^{\Delta x}, \mathbf{\Psi}^{\Delta x}) = 0 \tag{20}$$

for all $\mathbf{\Sigma}^{\Delta x} = (\mathbf{\Phi}^{\Delta x}, \mathbf{\Psi}^{\Delta x}) \in \mathcal{V}^k \times \mathcal{V}^k$.

Remark 5.2. *The method* (20) *is* consistent *for solving equation* (8) *if the true solution* $\mathbf{V}$ *is continuous and if* $\mathbf{B}(\mathbf{V})$ *depends continuously on* $\mathbf{V}$.

We can show the following result concerning entropy stability.

Theorem 5.1. *Consider the system* (8) *and let Assumption 5.1 hold true. Further assume that S is strictly convex. For simplicity, also assume that the exact and approximate solutions have compact support inside the spatial domain. Let the final time be denoted by t_-^N. Then, the approximate solutions generated by the scheme* (20) *satisfy*

$$\int_\Omega S(\mathbf{U}(\mathbf{V}^{\Delta x}(x, t_-^N)))\, dx + \int_{t^0}^{t^N} \int_\Omega (\mathbf{P}^{\Delta x})^2\, dx\, dt \leq \int_\Omega S(\mathbf{U}(\mathbf{V}^{\Delta x}(x, t_-^0)))\, dx.$$

Proof. We set $(\mathbf{\Phi}^{\Delta x}, \mathbf{\Psi}^{\Delta x}) = (\mathbf{V}^{\Delta x}, \mathbf{P}^{\Delta x})$ to get

$$0 = \mathcal{B}_{\text{ST}-\text{LDG}}(\mathbf{W}^{\Delta x}, \mathbf{W}^{\Delta x}) =$$

$$\mathcal{B}_{\text{DG}}(\mathbf{V}^{\Delta x}, \mathbf{V}^{\Delta x}) + \sum_{n,i} \int_{I^n} \int_{K_i} \langle \mathbf{P}^{\Delta x}, \mathbf{P}^{\Delta x} \rangle\, dx\, dt$$

$$+ \sum_{n,i} \int_{I^n} \int_{K_i} \left(\langle \mathbf{B}(\mathbf{V}^{\Delta x})\mathbf{P}^{\Delta x}, \mathbf{V}_x^{\Delta x} \rangle - \langle \mathbf{B}(\mathbf{V}^{\Delta x})\mathbf{V}_x^{\Delta x}, \mathbf{P}^{\Delta x} \rangle \right)\, dx\, dt$$

$$- \sum_{n,i} \int_{I^n} \left\langle \frac{\mathbf{B}(\mathbf{V}_{i+1/2,L}^{\Delta x}) + \mathbf{B}(\mathbf{V}_{i+1/2,R}^{\Delta x})}{2} \{\mathbf{P}^{\Delta x}\}_{i+1/2}, \mathbf{V}_{i+1/2,L}^{\Delta x} \right\rangle\, dt$$

$$+ \sum_{n,i} \int_{I^n} \left\langle \frac{\mathbf{B}(\mathbf{V}_{i-1/2,L}^{\Delta x}) + \mathbf{B}(\mathbf{V}_{i-1/2,R}^{\Delta x})}{2} \{\mathbf{P}^{\Delta x}\}_{i-1/2}, \mathbf{V}_{i-1/2,R}^{\Delta x} \right\rangle\, dt$$

$$- \frac{1}{2} \sum_{n,i} \int_{I^n} \left\langle \frac{\mathbf{B}(\mathbf{V}_{i+1/2,L}^{\Delta x}) + \mathbf{B}(\mathbf{V}_{i+1/2,R}^{\Delta x})}{2} [\mathbf{V}^{\Delta x}]_{i+1/2}, \mathbf{P}_{i+1/2,L}^{\Delta x} \right\rangle\, dt$$

$$- \frac{1}{2} \sum_{n,i} \int_{I^n} \left\langle \frac{\mathbf{B}(\mathbf{V}_{i-1/2,L}^{\Delta x}) + \mathbf{B}(\mathbf{V}_{i-1/2,R}^{\Delta x})}{2} [\mathbf{V}^{\Delta x}]_{i-1/2}, \mathbf{P}_{i-1/2,R}^{\Delta x} \right\rangle\, dt.$$

We examine the single terms, starting from below. Taking the symmetry of $\mathbf{B}$ and the compact support of the discrete solution into account, the boundary terms in the last four lines cancel each other. Also, the domain terms in the line above the boundary terms cancel each other. Let us now consider the terms in the first line. According to the proof of the entropy stability of the original scheme (compare also the proof of Theorem 4.1), there holds

$$\mathcal{B}_{\text{DG}}(\mathbf{V}^{\Delta x}, \mathbf{V}^{\Delta x}) \geq \int_\Omega S(\mathbf{U}(\mathbf{V}^{\Delta x}(x, t_-^N)))\, dx - \int_\Omega S(\mathbf{U}(\mathbf{V}^{\Delta x}(x, t_-^0)))\, dx.$$

This then directly implies the claim

$$\int_\Omega S(\mathbf{U}(\mathbf{V}^{\Delta x}(x, t_-^N)))\, dx + \int_{t^0}^{t^N} \int_\Omega (\mathbf{P}^{\Delta x})^2\, dx\, dt \leq \int_\Omega S(\mathbf{U}(\mathbf{V}^{\Delta x}(x, t_-^0)))\, dx.$$

$\square$

This concludes the description of the ST-LDG method. As a remark, in our method, we implement Dirichlet boundary conditions $\mathbf{U} = g$ on $\partial\Omega$ in the weak sense by setting $\mathbf{V}_{N+1/2,R}^{\Delta x} = \hat{\mathbf{g}}(x_{N+1/2})$ and $\mathbf{V}_{1/2,L}^{\Delta x} = \hat{\mathbf{g}}(x_{1/2})$, using appropriate boundary conditions $\mathbf{V} = \hat{\mathbf{g}}$ on $\partial\Omega$. Appropriate Dirichlet boundary conditions for $\mathbf{P}^{\Delta x}$ are deduced from the relation $\mathbf{P} = \mathbf{B}(\mathbf{V})\mathbf{V}_x$.

6. Numerical results

In this section we present various numerical results, comparing the ST-IP-DG and the ST-LDG method. For the ST-IP-DG method, we will also examine its dependence on the penalty parameter γ. In all our tests, the choice of the time step is purely based on the convection term, i.e., it does not take the presence of a diffusion term into account. We note that for stability reasons it is not necessary to restrict the time step due to the spacetime DG approach. But for accuracy reasons, we typically use the CFL condition

$$\Delta t^n \leq C_{\text{CFL}} \min_{x \in \Omega} \frac{\Delta x}{\lambda_{\max}(\mathbf{U}^{\Delta x}(x, t^n))}$$

with Δt^n denoting the time step from t^n to t^{n+1} and $C_{\text{CFL}} = 0.5$. We also use equidistant grid cells in our tests, but this is not necessary.

Our code is an extension of the one-dimensional version of SPARCCLE - the software package developed for the original scheme for hyperbolic conservation laws [17]. We refer to [17, 16] for more detailed information concerning the implementation and only give a short summary here.

The approximate solution $\mathbf{V}^{\Delta x} = (v_1^{\Delta x}, \ldots, v_m^{\Delta x})^T$ is sought in $\mathcal{V}^k$ with each component $v_j^{\Delta x}$ being of the form

$$v_j^{\Delta x} = \sum_{n,i,l} \hat{v}_{i,j,l}^n \phi_{i,l}^n$$

with n indicating the time segment, i the spatial cell, and $1 \leq l \leq n_f$ the degree of freedom depending on the choice of $\mathcal{V}^k$. Further, $\phi_{i,l}^n$ are basis functions with finite support given by

$$\phi_{i,l}^n\big|_{K_i \times I^n} = \left(\frac{t - t^{n+1}}{\Delta t^n}\right)^{k_{t,l}} \left(\frac{x - x_i}{\Delta x}\right)^{k_{x,l}}$$

with x_i denoting the centroid of the spatial cell i, and $k_{t,l} + k_{x,l} \leq k$. All spacetime and boundary integrals appearing in the numerical methods are evaluated using Gaussian quadrature formulae of the appropriate order.

While the form $\mathcal{B}_{\text{DG}}$ is non-linear in the discrete solution, it is linear in the test function. Therefore, it is sufficient to satisfy (3), the equation for conservation laws, for all basis functions of $\mathcal{V}^k$. Due to the choice of the upwind flux in time, one can solve each time step separately. All in all, in each time step, one needs to solve a non-linear system with $N_c \times n_f \times m$ unknowns, N_c denoting the number of spatial cells. Newton method with an analytically computed Jacobian is used for this purpose. For test problems in one dimension, it is typically sufficient to use a sparse LU decomposition in order to solve the linear problem in each Newton iteration. For the two-dimensional version of the code, suitable preconditioners have been developed to efficiently solve these subproblems [16].

In order to extend the code for conservation laws to convection-diffusion systems, only minor changes were necessary. Like for the original method, it is sufficient to satisfy equations (13) and (20) for all basis functions of $\mathcal{V}^k$. For the ST-IP-DG method, additional terms needed to be added in the evaluation of the residual and of the Jacobian of the non-linear system. For the ST-LDG method, we doubled the number of variables, and also adjusted the evaluation of the residual and of the Jacobian of the corresponding non-linear system. We have not yet examined whether it is possible to eliminate the auxiliary variables in the implementation,

which would result in a system corresponding to the size of the original variables (compare also the discussion in Section 7).

In the following, we will first show results for the scalar linear advection-diffusion equation. Then, in Section 6.2, we will present results for the compressible Navier-Stokes equations.

6.1. Numerical results for the linear advection-diffusion equation

We start with the linear advection-diffusion equation

$$\partial_t u + c \partial_x u = a \partial_x^2 u$$

with c and a constant (compare [7]). The initial data are chosen as

$$u(t = 0, x) = \sin(x)$$

on the domain $[0, 2\pi]$ with periodic boundary conditions. The exact solution is $u(t, x) = e^{-at} \sin(x - ct)$. We compute the solution up to $T = 2$ with parameters $a = 0.1$ and $c = 1$.

We use the quadratic entropy function $S(u) = \frac{1}{2} u^2$ and central flux for the entropy conservative flux $\mathbb{F}^*$, i.e., $\mathbb{F}^*(a, b) = \frac{1}{2}(a + b)$. We add Rusanov diffusion, which results in the numerical flux $\mathbb{F}$ corresponding to standard upwind flux.

Figure 1 shows the results for both the ST-IP-DG method, using $\gamma = 10$, and the ST-LDG for varying spaces $\mathcal{V}^k$, $k = 0, 1, 2, 3$. We note that the ST-IP-DG method does not converge for $\mathcal{V}^0$. This is consistent with the fact that for piecewise constant polynomials, most terms in the $\mathcal{B}_{\mathrm{IP}}$ form drop out and only the penalty term is left. The ST-LDG method converges with first order for $\mathcal{V}^0$. For $\mathcal{V}^k, k = 1, 2, 3$, the results for both methods are very comparable. In particular, both methods show the expected convergence order of $O(\Delta x^{k+1})$.

Next, we examine the dependence of the ST-IP-DG method on the penalty parameter γ. The stability condition for scalar equations is given by (17). In this fairly simple test, there holds $\underline{a} = \overline{a} = a$ and $m = M = 1$. Therefore, the stability condition requires that $1 - c_{\mathrm{inv}}\delta > 0$ and $\gamma > \frac{1}{\delta}$, i.e., that

$$\gamma > c_{\mathrm{inv}}.$$

Table 1: Lin. adv.-diff. eqn.: Influence of γ on the stability of the ST-IP-DG method. '$\times$' denotes an unstable test, '$\checkmark$' a stable one.

	$\mathcal{V}^1$	$\mathcal{V}^2$	$\mathcal{V}^3$
$\gamma = 0.1$	$\times$	$\times$	$\times$
$\gamma = 1$	$\checkmark$	$\times$	$\times$
$\gamma = 10$	$\checkmark$	$\checkmark$	$\checkmark$

Numerically, we observe the results shown in Table 6.1. This is consistent with our theoretical stability considerations that for $\mathcal{V}^1$ polynomials the inverse estimate holds for our polynomials with $c_{\mathrm{inv}} = 1$, whereas for $\mathcal{V}^2$ and $\mathcal{V}^3$ the constant c_{inv} cannot be smaller than 3.

Figure 2 shows the influence of the parameter γ on the accuracy of the method. In the case of the space $\mathcal{V}^1$, there is a significant difference in accuracy between choosing $\gamma = 10$ and $\gamma = 1000$. For $\mathcal{V}^2$, all results are very similar. The results for $\mathcal{V}^1$ are quite untypical. In most of our tests there was only a small dependence of the accuracy on the parameter γ. Overall, choosing $\gamma = 10$ seemed to be a good default choice.

6.2. Numerical results for the compressible Navier-Stokes equations

In this section, we solve the compressible Navier-Stokes equations in one dimension given by (9) with Dirichlet boundary conditions and $\gamma = 1.4$. (Here, γ refers to the adiabatic exponent

17

Figure 1: Lin. adv.-diff. eqn.: Comparison of the ST-IP-DG method with $\gamma = 10$ (dashed lines) and the ST-LDG method (solid lines). (For $\mathcal{V}^2$, the results for ST-IP-DG and ST-LDG almost coincide.)

(a) $\mathcal{V}^1$

(b) $\mathcal{V}^2$
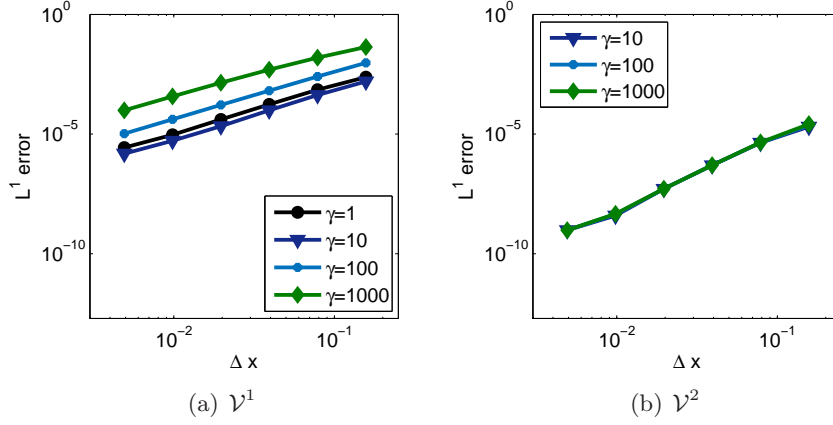
Figure 2: Lin. adv.-diff. eqn.: Influence of γ on the accuracy of the ST-IP-DG method. (The choice $\gamma = 1$ was not stable for $\mathcal{V}^2$.)

in the compressible Navier-Stokes equations.) We follow [19] for the entropy conservative flux $\mathbb{F}^*$ for the convection terms. Entropy stable flux is attained by adding the Rusanov diffusion operator.

Remark 6.1. *In the following we will show several comparisons for the ST-IP-DG and the ST-LDG method for various polynomials degrees. Since the ST-IP-DG method is not consistent for $\mathcal{V}^0$, we do not include these results in the plots in this section. However, we do show results for the ST-LDG method for using $\mathcal{V}^0$. All tests for the ST-IP-DG method use $\gamma = 10$.*
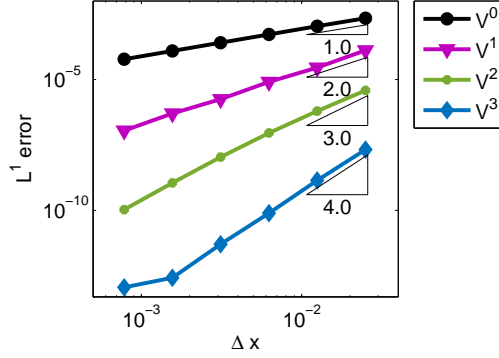
Figure 3: Manufactured solution: Comparison of the ST-IP-DG method (dashed lines) and the ST-LDG method (solid lines) using entropy stable flux. (For $\mathcal{V}^1$, $\mathcal{V}^2$, and $\mathcal{V}^3$, the results for ST-IP-DG and ST-LDG are almost identical.)

6.2.1. Manufactured solution

We start with a test that has a manufactured solution. To assess the accuracy of our methods, we like the solution to be given by the smooth functions

$$\rho(x,t) = \sin(x^2 + 5t) + 1.5,$$
$$u(x,t) = 2\left[\sin(x^2 + 5t) + 0.1\right],$$
$$e(x,t) = 3\left[\cos(x^2 + 5t) + 1.5\right].$$

We insert this solution into the compressible Navier-Stokes equations and compute the corresponding source terms that need to be added on the right hand side of the equations to render the above triple (ρ, u, e) a solution of the resulting equations. We use the viscosity coefficient $\nu = 2 \cdot 10^{-5}$ and entropy stable flux. The test domain is given by $\Omega = [-0.1; 0.9]$ and the final time is $T = 0.05$.

Figure 3 shows the error in density for both the ST-IP-DG and the ST-LDG method. The results are almost identical for $\mathcal{V}^1$, $\mathcal{V}^2$, and $\mathcal{V}^3$. For all tested polynomial degrees we observe the expected convergence order of $O(\Delta x^{k+1})$ for $\mathcal{V}^k$, confirming the arbitrarily high order of our methods for smooth solutions. The results for momentum and energy are qualitatively the same.

Next, we consider the situation for entropy conservative flux. Figure 4 shows the comparison of the two methods for the error in density. We observe a decay in accuracy for both methods for using polynomial spaces of odd degrees. A similar behavior has been observed by other authors [7, 3]. Overall both methods are very comparable.

6.2.2. Modified Sod test

Our next test is a modified Sod problem, similar to the test in [27]. We consider initial data

$$(\rho, m, E) = \begin{cases} (1.0, 0.0, 2.5) & \text{if } x < 0, \\ (0.125, 0.0, 0.25) & \text{if } x > 0, \end{cases}$$

on the domain $\Omega = [-0.5, 0.5]$. The viscosity $\nu = 2.5 \cdot 10^{-5}$ is fairly small.
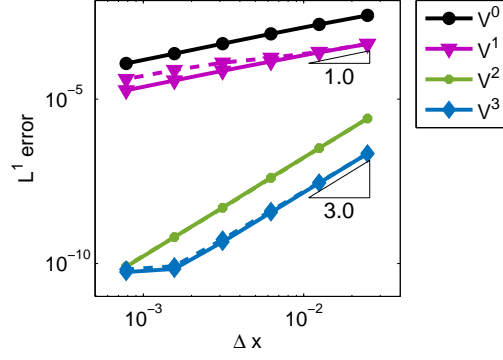
Figure 4: Manufactured solution: Comparison of the ST-IP-DG method (dashed lines) and the ST-LDG method (solid lines) using entropy conservative flux. (For $\mathcal{V}^2$, the results for ST-IP-DG and ST-LDG are very similar.)

(a) Density ρ for $\Delta x = 1.0 \cdot 10^{-2}$

(b) Density ρ for $\Delta x = 2.5 \cdot 10^{-4}$

(c) Velocity u for $\Delta x = 1.0 \cdot 10^{-2}$

(d) Velocity u for $\Delta x = 2.5 \cdot 10^{-4}$
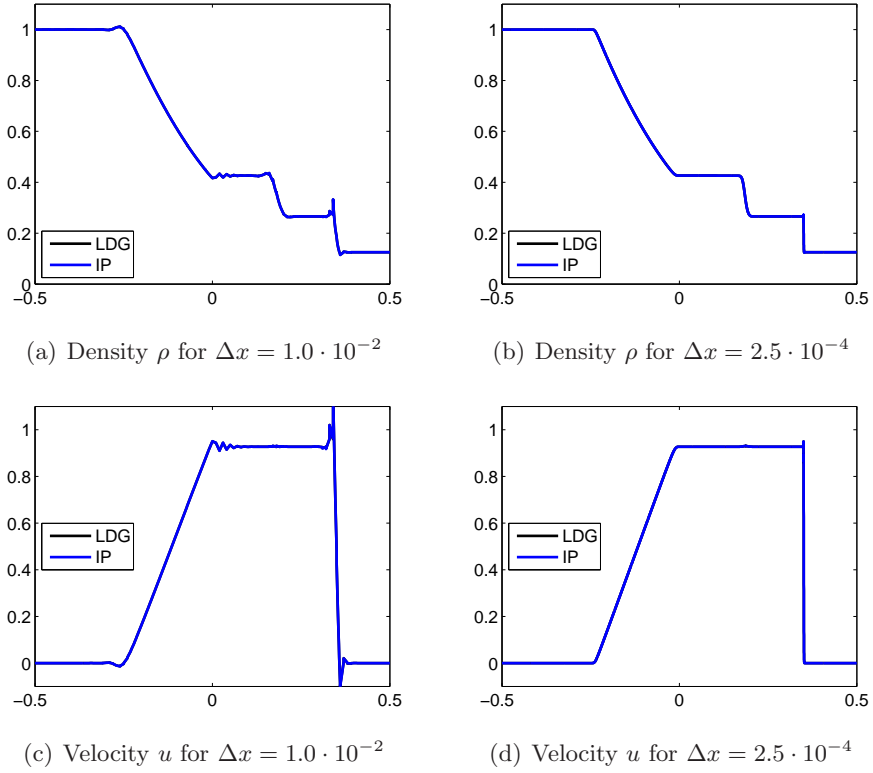
Figure 5: Modified Sod test: Comparison of the ST-IP-DG and the ST-LDG method using entropy stable flux and $\mathcal{V}^1$. (The solutions for ST-IP-DG and ST-LDG almost coincide.)

(a) Density ρ for $\Delta x = 1.0 \cdot 10^{-2}$ (b) Density ρ for $\Delta x = 2.5 \cdot 10^{-4}$

(c) Velocity u for $\Delta x = 1.0 \cdot 10^{-2}$ (d) Velocity u for $\Delta x = 2.5 \cdot 10^{-4}$
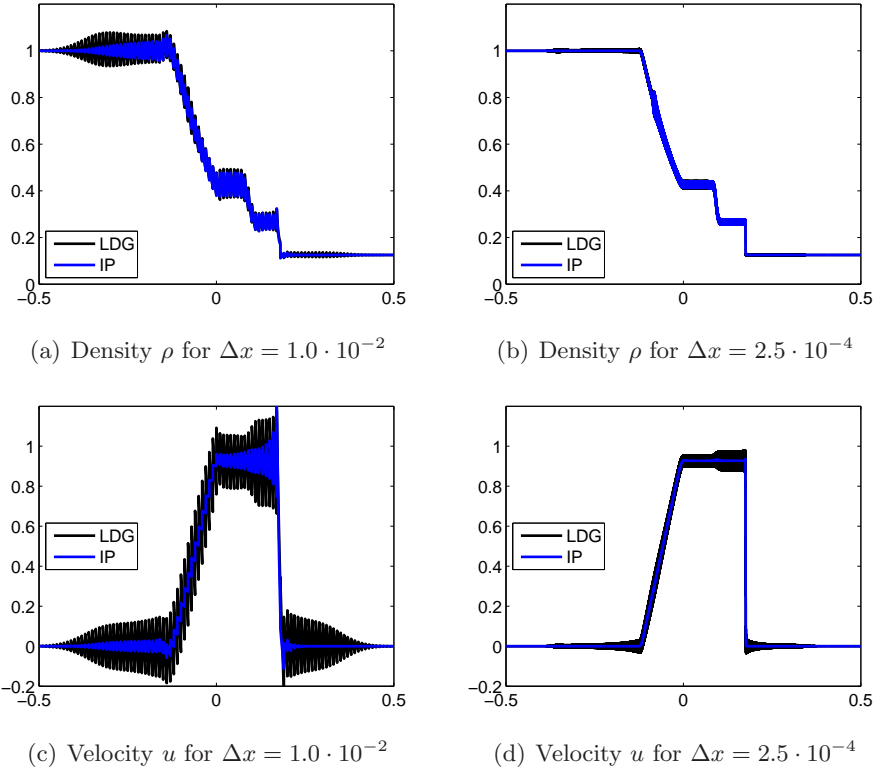
Figure 6: Modified Sod test: Comparison of the ST-IP-DG and the ST-LDG method using entropy conservative flux and $\mathcal{V}^1$.

(a) entropy stable flux   (b) entropy conservative flux
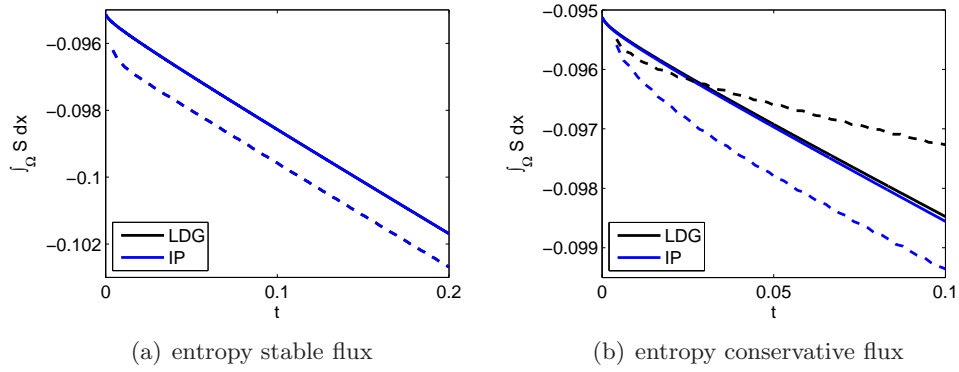
Figure 7: Modified Sod test: Comparison of the behavior of $\int_\Omega S\,dx$ over time. The dashed lines correspond to coarse grid solutions with $\Delta x = 1.0 \cdot 10^{-2}$ and the solid lines to fine grid solutions with $\Delta x = 2.5 \cdot 10^{-4}$. (For entropy stable flux, the results for the ST-IP-DG method and the ST-LDG method are very similar.)

Figure 5 shows the results for $\mathcal{V}^1$ using entropy stable flux with final time $T = 0.20$. The results for the ST-IP-DG and the ST-LDG method are almost identical. For both methods, we observe oscillations in the solution around the contact discontinuity and the shock for the coarse mesh with $\Delta x = 1.0 \cdot 10^{-2}$. For this mesh size, the physical viscosity of the compressible Navier-Stokes equations cannot be resolved. In the original method [17], streamline diffusion and shock capturing operators $\mathcal{B}_{\text{SD}}$ and $\mathcal{B}_{\text{SC}}$ are employed to avoid these oscillations. On the finer grid with $\Delta x = 2.5 \cdot 10^{-4}$, however, the oscillations have vanished: if the mesh width is chosen fine enough, there is no need to add operators like $\mathcal{B}_{\text{SD}}$ and $\mathcal{B}_{\text{SC}}$.

Next, we consider the same test with entropy conservative flux and with final time $T = 0.10$. The results for $\mathcal{V}^1$ for both methods are shown in Figure 6. In this case, we observe significant oscillations and different behavior of the ST-IP-DG and the ST-LDG method. The latter one leads to bigger oscillations in the solution, indicating that the method may be less diffusive.

To follow up on this suspicion, we evaluate $\int_{\Omega} S dx$ at the end of each time step for both methods on the coarse grid and on the fine grid. The result is shown in Figure 7. We make the following observations.

- For entropy *stable* flux, the behavior of the entropy over time is the same for the ST-IP-DG as for the ST-LDG method. This is consistent with the solution plots in Figure 5 in the sense that the solutions for both methods are very similar. Apparently, potential differences are annihilated by adding the Rusanov diffusion.

- For entropy *conservative* flux, we observe less entropy decay when using the ST-LDG method than when using the ST-IP-DG method, especially for the coarse grid. This is consistent with the ST-LDG method resulting in more excessive oscillations in the solutions as shown in Figure 6.

Remark 6.2. *We note that we do not expect conservation of entropy when using entropy conservative flux due to the viscosity and heat conduction terms present in the equations. This is also a likely explanation for why the ST-LDG method leads to less entropy decay on the coarse grid than on the fine grid: the coarse grid cannot sufficiently resolve the viscosity in the system.*

6.2.3. Modified Shu-Osher test

Finally, to test the robustness of our scheme, we use a modified Shu-Osher test. We consider initial data

$$(\rho, u, p) = \begin{cases} (3.857143, 2.629369, 10.33333) & \text{if } x < -4.0, \\ (1 + 0.2\sin(5.0x), 0.0, 1.0) & \text{if } x > -4.0, \end{cases}$$

on the domain $\Omega = [-5, 5]$ with final time $T = 1.8$. The viscosity is chosen as $\nu = 4.0 \cdot 10^{-3}$ and we use entropy stable flux.

Figure 8 shows the solution for $\mathcal{V}^2$ for both methods for two different grid sizes. Again, we observe that the results for the ST-IP-DG method and the ST-LDG method are almost identical. For both methods, the viscosity $\nu = 4.0 \cdot 10^{-3}$ cannot fully be resolved for the coarse grid size $\Delta x = 1.0 \cdot 10^{-2}$, resulting in overshoot in the solution. This is not the case for the fine grid size with $\Delta x = 4.0 \cdot 10^{-3}$.

This completes the presentation of our numerical results. We conclude this work with a direct comparison of the ST-IP-DG and the ST-LDG method.
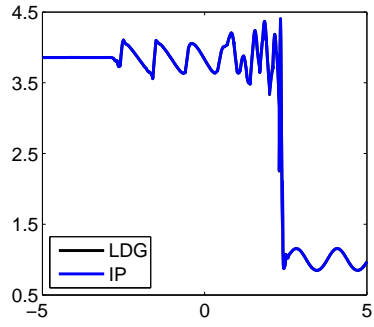
(a) Density ρ for $\Delta x = 1.0 \cdot 10^{-1}$
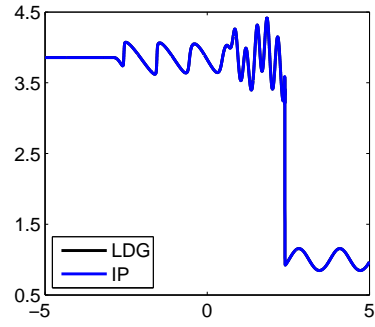
(b) Density ρ for $\Delta x = 4.0 \cdot 10^{-3}$
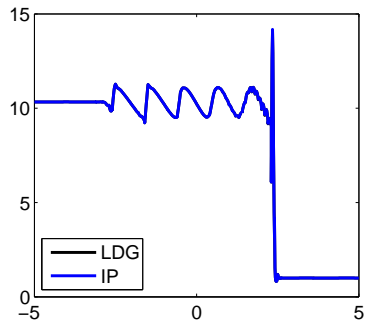
(c) Pressure p for $\Delta x = 1.0 \cdot 10^{-1}$
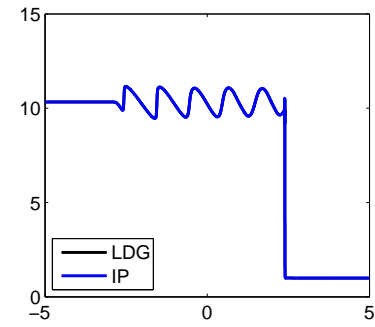
(d) Pressure p for $\Delta x = 4.0 \cdot 10^{-3}$

Figure 8: Modified Shu-Osher test: Comparison of the ST-IP-DG and the ST-LDG method using entropy stable flux and $\mathcal{V}^2$. (The solutions for both methods are similar.)

7. Comparison of the ST-IP-DG and the ST-LDG method

Both methods satisfy the main features we were looking for: both schemes are fully discrete, unconditionally stable, and (arbitrarily) high order as confirmed by the numerical results. Furthermore, we have shown entropy stability for both the ST-IP-DG method and the ST-LDG method in Theorems 4.1 and 5.1, even though stronger assumptions are needed for the ST-IP-DG method. Therefore, both methods are suitable candidates for the extension to two dimensions. Which one is more suitable?

In a direct comparison of the schemes we make the following observations:

- ***Accuracy:*** Overall, both schemes lead to very similar numerical results, especially when entropy stable flux is used.

- ***Penalty parameter:*** The ST-IP-DG method involves the penalty parameter γ. Based on the stability analysis, the size of the parameter depends on the actual problem, making its choice difficult. However, in our numerical tests, the default choice $\gamma = 10$ worked very well.

- ***Cost/Implementation:*** For the ST-IP-DG method, additional terms need to be added to the original scheme for hyperbolic conservation laws. For the ST-LDG method, one needs to introduce additional variables $\mathbf{P}$. In the case of the compressible Navier-Stokes equations in one dimension, this increases the number of variables from 3 to 5 (due to the special structure of the matrix $\mathbf{A}$). In each iteration of the Newton method, a linear system of the size $(m \times n_f \times N_c)^2$ must be solved. Depending on the solver used in this step, the increase in number of variables will result in a multiplied increase in cost. Also, a suitable matrix $\mathbf{B}$ needs to be found for the method to work.

Overall, the ST-LDG method has better theoretical properties as it does not involve a penalty parameter and uses a weaker assumption in the entropy stability theorem. Computationally, however, the method is only competitive to the ST-IP-DG method if it is possible to eliminate the additional variables by using, e.g., lift operators, which is common practice for the LDG method. Also, it will be relevant whether the lift operator will lead to a coupling of cells that are not direct neighbors. The CDG method [22] was developed as a response to the original LDG method having that issue. If good solutions for these two problems for the ST-LDG method can be developed in two and three dimensions, then the ST-LDG method is preferable.

Acknowledgments

A. Boundary terms for the ST-IP-DG method

We now describe the ST-IP-DG method for solving the system (8) with non-homogeneous Dirichlet boundary conditions $\mathbf{U} = \mathbf{g}$ on $\partial\Omega$. Instead of (13), one needs to solve the system

$$\mathcal{B}_{\text{DG}}(\mathbf{V}^{\Delta x}, \mathbf{\Phi}^{\Delta x}) + \mathcal{B}_{\text{IP}}(\mathbf{V}^{\Delta x}, \mathbf{\Phi}^{\Delta x}) = \mathcal{B}_{\text{RHS}}(\mathbf{\Phi}^{\Delta x}). \tag{21}$$

The definition of $\mathcal{B}_{\mathrm{IP}}$ for interior edges is given by (14). For boundary edges, some terms need to be modified. Also, because some terms in the definition of $\mathcal{B}_{\mathrm{IP}}$ do not arise naturally by, e.g., integration by parts but are added to the form, these terms need to be compensated for on the right hand side of the equation in form of $\mathcal{B}_{\mathrm{RHS}}$.

Let us focus on the left domain boundary with the spatial cells being numbered from 1 to N. Then, the left-most cell has edges located at $x_{1/2}$ and $x_{3/2}$. By our standard change of variables, the Dirichlet boundary conditions $\mathbf{U} = \mathbf{g}$ on $\partial\Omega$ correspond to $\mathbf{V} = \hat{\mathbf{g}}$ on $\partial\Omega$. Then the edge terms in the form $\mathcal{B}_{\mathrm{IP}}(\mathbf{V}^{\Delta x}, \mathbf{\Phi}^{\Delta x})$ need to be adjusted in the following way at the left domain boundary (using $\hat{\mathbf{g}} = \hat{\mathbf{g}}(x_{1/2})$)

$$\int_{I_n} \langle \mathbf{A}(\{\mathbf{V}^{\Delta x}\}) \{\mathbf{V}^{\Delta x}_x\}_{1/2}, [\mathbf{\Phi}^{\Delta x}]_{1/2} \rangle \, dt \quad \rightarrow \quad \int_{I_n} \langle \mathbf{A}(\hat{\mathbf{g}})(\mathbf{V}^{\Delta x}_x)_{1/2,R}, \mathbf{\Phi}^{\Delta x}_{1/2,R} \rangle \, dt,$$

$$\int_{I_n} \langle \mathbf{A}(\{\mathbf{V}^{\Delta x}\})[\mathbf{V}^{\Delta x}]_{1/2}, \{\mathbf{\Phi}^{\Delta x}_x\}_{1/2} \rangle \, dt \quad \rightarrow \quad \int_{I_n} \langle \mathbf{A}(\hat{\mathbf{g}})\mathbf{V}^{\Delta x}_{1/2,R}, (\mathbf{\Phi}^{\Delta x}_x)_{1/2,R} \rangle \, dt,$$

$$\int_{I_n} \frac{\gamma}{\Delta x} \langle \mathbf{A}(\{\mathbf{V}^{\Delta x}\})[\mathbf{V}^{\Delta x}]_{1/2}, [\mathbf{\Phi}^{\Delta x}]_{1/2} \rangle dt \quad \rightarrow \quad \int_{I_n} \frac{\gamma}{\Delta x} \langle \mathbf{A}(\hat{\mathbf{g}})\mathbf{V}^{\Delta x}_{1/2,R}, \mathbf{\Phi}^{\Delta x}_{1/2,R} \rangle dt.$$

Similar modifications, using $\mathbf{\Phi}^{\Delta x}_{N+1/2,L}$ and $(\mathbf{\Phi}^{\Delta x}_x)_{N+1/2,L}$, are necessary at the right domain boundary. Additionally, one needs to compensate for the additional terms in the form $\mathcal{B}_{\mathrm{IP}}$ that did not arise by integration by parts on the right hand side of equation (21) by means of $\mathcal{B}_{\mathrm{RHS}} = \mathcal{B}^{1/2}_{\mathrm{RHS}} + \mathcal{B}^{N+1/2}_{\mathrm{RHS}}$ with

$$\mathcal{B}^{1/2}_{\mathrm{RHS}}(\mathbf{\Phi}^{\Delta x}) = \int_{I_n} \langle \mathbf{A}(\hat{\mathbf{g}})\hat{\mathbf{g}}, (\mathbf{\Phi}^{\Delta x}_x)_{1/2,R} \rangle \, dt + \int_{I_n} \frac{\gamma}{\Delta x} \langle \mathbf{A}(\hat{\mathbf{g}})\hat{\mathbf{g}}, \mathbf{\Phi}^{\Delta x}_{1/2,R} \rangle dt.$$

B. Using the ST-LDG method for solving the compressible Navier-Stokes equations

The ST-LDG method is based on the existence of a positive semi-definite matrix $\mathbf{B}(\mathbf{V})$ such that $\mathbf{B}^2 = \mathbf{A}$ with $\mathbf{A}$ given by (8). In the following we describe the matrix $\mathbf{B}$ that we use in our numerical tests for the compressible Navier-Stokes equations.

Instead of decomposing the matrix $\mathbf{A}$ we decompose the reduced matrix $\tilde{\mathbf{A}}$ given by (11). We can write $\tilde{\mathbf{A}} = \mathbf{C}\mathbf{\Lambda}\mathbf{C}^{-1}$ with the matrix $\mathbf{\Lambda} = \mathrm{diag}(\lambda_1, \lambda_2)$ containing the positive eigenvalues of $\tilde{\mathbf{A}}$ and the columns of $\mathbf{C}$ containing the corresponding eigenvectors. We use this to define $\mathbf{B} = \mathbf{C}\mathbf{\Lambda}^{1/2}\mathbf{C}^{-1}$. In our tests we use

$$\mathbf{C} = \begin{pmatrix} \frac{1}{N_1}\left(\lambda_1 + \nu\frac{v_2^2}{v_3^3} - \frac{\kappa}{R}\frac{1}{v_3^2}\right) & \frac{1}{N_2} \cdot \nu\frac{v_2}{v_3^2} \\ \frac{1}{N_1} \cdot \nu\frac{v_2}{v_3^2} & \frac{1}{N_2}\left(\lambda_2 + \frac{\nu}{v_3}\right) \end{pmatrix}$$

with N_1 and N_2 representing the appropriate normalization factors given by

$$N_1 = \sqrt{\left(\lambda_1 + \nu\frac{v_2^2}{v_3^3} - \frac{\kappa}{R}\frac{1}{v_3^2}\right)^2 + \left(\nu\frac{v_2}{v_3^2}\right)^2} \quad \text{and} \quad N_2 = \sqrt{\left(\nu\frac{v_2}{v_3^2}\right)^2 + \left(\lambda_2 + \frac{\nu}{v_3}\right)^2}.$$

References

[1] D. N. Arnold. An interior penalty finite element method with discontinuous elements. *SIAM J. Numer. Anal.*, 19:742–760, 1982.

[2] D. N. Arnold, F. Brezzi, B. Cockburn, and L. D. Marini. Unified analysis of discontinuous Galerkin methods for elliptic problems. *SIAM J. Numer. Anal.*, 39:1749–1779, 2002.

[3] P. Aursand and U. Koley. Higher-order energy stable schemes for a nonlinear variational wave equation modeling nematic liquid crystals in two dimensions. Submitted.

[4] F. Bassy and S. Rebay. A high-order accurate discontinuous finite element method for the numerical solution of the compressible Navier-Stokes equations. *J. Comput. Phys.*, 131:267–279, 1997.

[5] F. Bassy, S. Rebay, G. Mariotti, S. Pedinotti, and M. Savini. A high-order accurate discontinuous finite element method for inviscid turbomachinery flows. In *Proceedings of the 2nd European Conference on Turbomachinery Fluid Dynamics and Thermodynamics*, pages 99–108, 1997. Antwerp, Belgium.

[6] S. Brdar, A. Dedner, and R. Klöfkorn. Compact and stable discontinuous Galerkin methods for convection-diffusion problems. *SIAM J. Sci. Comput.*, 34:A263–A282, 2012.

[7] B. Cockburn and C.-W. Shu. The local discontinuous Galerkin method for time-dependent convection-diffusion systems. *Siam J. Numer. Anal.*, 35:2440–2463, 1998.

[8] U. S. Fjordholm, S. Mishra, and E. Tadmor. Energy preserving and energy stable schemes for the shallow water equations. In *Foundations of Computational Mathematics*, pages 93–139, 2009. London Math. Soc. Lecture Notes Ser. 363.

[9] U. S. Fjordholm, S. Mishra, and E. Tadmor. Arbitrarily high order accurate entropy stable essentially non-oscillatory schemes for systems of conservation laws. *SIAM J. Numer. Anal.*, 50:544–573, 2012.

[10] K. O. Friedrichs and P. D. Lax. Systems of conservation laws with a convex extension. *Proc. Nat. Acad. Sci. U.S.A.*, 68:1686–1688, 1971.

[11] S. K. Godunov. An interesting class of quasilinear systems. *Dokl. Acad. Nauk. SSSR*, 139:521–523, 1961.

[12] A. Harten. On the symmetric form of systems of conservation laws with entropy. *J. Comput. Phys.*, 49:151–164, 1983.

[13] A. Harten and P. D. Lax. A random choice finite difference scheme for hyperbolic conservation laws. *SIAM J. Numer. Anal.*, 18:289–315, 1981.

[14] R. Hartmann and P. Houston. Symmetric interior penalty DG methods for the compressible Navier-Stokes equations I: Method formulation. *Int. J. Numer. Anal. Model*, 3:1–20, 2006.

[15] R. Hartmann and P. Houston. An optimal order interior penalty discontinuous Galerkin discretization of the compressible Navier-Stokes equations. *J. Comput. Phys.*, 227:9670–9685, 2008.

[16] A. Hiltebrand and S. Mishra. Efficient preconditioners for a shock capturing space-time discontinuous Galerkin method for systems of conservation laws. Technical Report 2014-04, Seminar for Applied Mathematics, ETH Zürich, 2014.

[17] A. Hiltebrand and S. Mishra. Entropy stable shock capturing space-time discontinuous Galerkin schemes for systems of conservation laws. *Numer. Math.*, 126:103–151, 2014.

[18] T. J. R. Hughes, L. P. Franca, and M. Mallet. A new finite element formulation for computational fluid dynamics: I. Symmetric forms of the compressible Euler and Navier-Stokes equations and the second law of thermodynamics. *Comput. Methods Appl. Mech. Engrg.*, 54:223–234, 1986.

[19] F. Ismail and P. L. Roe. Affordable, entropy-consistent Euler flux functions II: Entropy production at shocks. *J. Comput. Phys.*, 228:5410–5436, 2009.

[20] M. S. Mock. Systems of conservations laws of mixed type. *J. Differential Equations*, 37:70–88, 1980.

[21] J.A. Nitsche. Über ein Variationsprinzip zur Lösung von Dirichlet-Problemen bei Verwendung von Teilräumen, die keinen Randbedingungen unterworfen sind. *Abh. Math. Sem. Univ. Hamburg.*, 36:9–15, 1971.

[22] J. Peraire and P.-O. Persson. The compact discontinuous Galerkin (CDG) method for elliptic equations. *SIAM J. Sci. Comput.*, 30:1908–1824, 2008.

[23] P.-O. Persson and J. Peraire. Newton-GMRES preconditioning for discontinuous Galerkin discretizations of the Navier-Stokes equations. *SIAM J. Sci. Comput.*, 30:2709–2733, 2008.

[24] B. Rivière. *Discontinuous Galerkin Methods for solving elliptic and parabolic equations: Theory and implementation.* SIAM, 2008.

[25] F. Shakib, T. J. R. Hughes, and Z. Johan. A new finite element formulation for computational fluid dynamics: X. The compressible Euler and Navier-Stokes equations. *Comput. Methods Appl. Mech. Engrg.*, 89:141–219, 1991.

[26] E. Tadmor. The numerical viscosity of entropy stable schemes for systems of conservation laws. *Math. Comp.*, 49:91–103, 1987.

[27] E. Tadmor and W. Zhong. Entropy stable approximations of Navier-Stokes equations with no artificial numerical viscosity. *J. Hyperbolic Differ. Equ.*, 3:529–559, 2006.

Recent Research Reports

Nr.	Authors/Title

2014-35   P. Grohs and A. Obermeier
Ridgelet Methods for Linear Transport Equations

2014-36   P. Chen and Ch. Schwab
Sparse-Grid, Reduced-Basis Bayesian Inversion

2014-37   R. Kaeppeli and S. Mishra
Well-balanced schemes for gravitationally stratified media

2014-38   D. Schoetzau and Ch. Schwab
Exponential Convergence for hp-Version and Spectral Finite Element Methods for
Elliptic Problems in Polyhedra

2014-39   P. Grohs and M. Sprecher
Total Variation Regularization by Iteratively Reweighted Least Squares on Hadamard
Spaces and the Sphere

2014-40   R. Casagrande and R. Hiptmair
An A Priori Error Estimate for Interior Penalty Discretizations of the Curl-Curl
Operator on Non-Conforming Meshes

2015-01   X. Claeys and R. Hiptmair
Integral Equations for Electromagnetic Scattering at Multi-Screens

2015-02   R. Hiptmair and S. Sargheini
Scatterers on the substrate: Far field formulas

2015-03   P. Chen and A. Quarteroni and G. Rozza
Reduced order methods for uncertainty quantification problems

2015-04   S. Larsson and Ch. Schwab
Compressive Space-Time Galerkin Discretizations of Parabolic Partial